

OVERVIEW NO. 98

I—GEOMETRIC MODELS OF CRYSTAL GROWTH

J. E. TAYLOR¹, J. W. CAHN² and C. A. HANDWERKER²

¹Mathematics Department, Rutgers University, New Brunswick, NJ 08903 and

²National Institute of Standards and Technology, Gaithersburg, MD 20899, U.S.A.

(Received 18 October 1991)

Abstract—Recent theoretical advances in the mathematical treatment of *geometric* interface motion make more tractable the theory of a wide variety of materials science problems where the interface velocity is not controlled by long-range-diffusion. Among the interface motion problems that can be modelled as geometric are certain types of phase changes, crystal growth, domain growth, grain growth, ion beam and chemical etching, and coherency stress driven interface migration. We provide an introduction to nine mathematical methods for solving such problems, give the limits of applicability of the methods, and discuss the relations among them theoretically and their uses in computation. Comparisons of some of them are made by displaying how the same physical problems are treated in the various applicable methods.

Résumé—Des progrès théoriques récents dans le traitement mathématique du mouvement de l'interface *géométrique* rendent plus abordable la théorie d'un grand nombre de problèmes de science des matériaux où la vitesse de l'interface n'est pas contrôlée par la diffusion à longue distance. Parmi les problèmes de mouvement d'interface qui peuvent être modélisés d'une manière géométrique il y a certains types de transitions de phases, de croissance cristalline, de croissance de domaines, de croissance de grains, de corrosion par bombardement ionique et de corrosion chimique et de migration de l'interface pilotée par la contrainte de cohérence. Nous donnons une introduction relative à neuf méthodes mathématiques pour résoudre de tels problèmes; nous donnons les limites d'application de ces méthodes et nous discutons d'une manière théorique les relations entre celles-ci ainsi que leurs utilisations dans les calculs. Des comparaisons entre certaines de ces méthodes sont effectuées en montrant comment les mêmes problèmes physiques sont traités par les différentes méthodes applicables.

Zusammenfassung—Neuere theoretische Fortschritte in der mathematischen Behandlung *geometrischer* Grenzflächenbewegungen machen die Theorie einer großen Vielzahl von werkstoffwissenschaftlichen Problemen, in denen die Grenzflächengeschwindigkeit nicht gesteuert ist von weitreichender Diffusion, traktabel. Unter den als geometrisch zu behandelnden Problemen der Grenzflächenbewegung fallen gewisse Typen von Phasenänderungen, Kristallwachstum, Domänenwachstum, Kornwachstum, Ionenstrahl- und chemische Ätzung und durch Kohärenzspannungen angetriebene Grenzflächenwanderung. Wir legen eine Einführung in neun mathematische Methoden zur Lösung dieser Probleme vor, beschreiben die Anwendungsgrenzen dieser Methoden und diskutieren die Zusammenhänge zwischen ihnen theoretisch und die Nützlichkeit bei Computerrechnungen. Einige werden miteinander verglichen, indem dieselben physikalischen Probleme mit den verschiedenen anwendbaren Methoden behandelt werden.

1. INTRODUCTION

There have been considerable recent theoretical advances in certain mathematical problems of surface motion, those that are called *geometric* [1–33]. (See the Glossary in the Appendix for all italicized words.) *Geometric* means that the normal velocity v of the surface depends only on the position and local shape of the surface. The velocity can also depend on the values that field variables, such as temperature and concentration, take on the surface if these values are not modified by diffusion, but it cannot depend on variables away from the surface, such as concentration gradients created by surface motion and modified by diffusion in the bulk. For example, in a *geometric* surface motion problem, v might

depend only on the direction of the local normal \mathbf{n} and/or the local components of the curvature, which are given by the spatial derivatives of \mathbf{n} ; v could also depend on position and thus the local microstructure or fixed temperature field. In *geometric* surface motion problems, v can depend on time implicitly through the time dependence of the temperature and concentration; an explicit dependence on time is also allowed mathematically.

Geometric crystal growth is a very active area of theoretical and computational research, and a fast-moving field. We have attempted to provide an introduction to nine mathematical methods for solving such problems, say what relations that are between them theoretically, and compare some of them by displaying how the same physical problems

are treated in the various applicable methods. This survey has been aimed primarily towards materials scientists and physicists interested in the problem of interface motion. As we described in a previous paper [2] and below, there are many examples in materials science where surface or interface motion can be simplified to fit a geometric model. This paper is not intended to be an outline of mathematical proofs, nor a statement of precise mathematical results, nor even a preparation for proving further mathematical results. For these, one must go to the original papers.

In geometric models of interface motion we will usually take v to depend on a thermodynamic driving force that is the free energy decrease (per unit magnitude volume change) if the surface were to move to increase the volume of the phase behind it. This driving force has two components, a weighted mean curvature (wmc) that expresses the decrease in the integral of the specific surface free energy γ and a volume phase change part Ω . It is convenient to define a non-negative mobility function M as the ratio of v to driving force, so that

$$v = M(\Omega + wmc).$$

Because the sign of v must be such that the free energy decreases, M must be non-negative, but otherwise M , Ω , and wmc can be complicated functions of all the remaining factors that enter into the geometric problem [13], including factors like temperature, orientation and microstructure. Since v need not depend linearly on the driving force, M can even depend on v itself. Most of the recent mathematical progress has been in the linear response case where

$$v = M(\mathbf{x}, t, \mathbf{n})[\Omega(\mathbf{x}, t) + wmc(\mathbf{x}, t)]$$

The various forms that wmc can take are summarized in the companion paper [34] and are also given as needed in the descriptions of various formulations in Sections 2 and 3. If we want a model that ignores curvature, we can accomplish this by setting the surface free energy γ equal to zero on all unit vectors.

There are many examples in materials science where surface or interface motion can be simplified to fit a geometric model. (We use the word "surface" to denote an interface between crystals including crystals of the same phase but different crystallographic orientations as well as one between a crystal and a fluid.) Interface-controlled crystal growth or dissolution, chemical and ion etching, domain and grain growth, liquid film migration, diffusion-induced grain boundary motion, eutectic growth, cellular precipitation, and discontinuous coarsening are examples of such phenomena. Two dimensional examples are dislocation motion on a slip plane, and spreading of new layers during growth of a faceted crystal.

Complications which can make these processes non-geometric include temperature and/or concentration profiles that depend on the motion, as in diffusion controlled crystal and dendrite growth. Certain diffusion problems, however, can be formulated as geometric. In these a local steady state in the framework of the moving surface leads to gradients that are constant in time, and therefore a v that is also independent of time. The velocity may be a function of \mathbf{n} and its gradients. Eutectic growth can be an example, in which the phases grow as parallel lamella or rods in which the spacings and the diffusion profiles ahead of the interfaces become constant; the average velocity of the corrugated two-phase growth front is constant in time, but may depend on the average orientation of the surface. In coherency stress driven processes, such as liquid film migration and diffusion-induced grain boundary migration, there is a steady state diffusion field ahead of the interface. Cellular precipitation and eutectoid growth can also be steady-state diffusion processes, in which the diffusion field creates both the necessary fluxes for the separation of the elements into the two phases, and the coherency stresses that may also be a factor in the driving force for surface migration.

When the rate of crystal growth or dissolution is said to be controlled by interface processes, interface motion is so slow that the diffusion of mass or heat has little or no effect on the kinetics [35], or else there is nothing to diffuse away (as in phase-antiphase boundary migration [36, 37]). The rate v is then entirely controlled by molecular processes at the interface, and these in turn depend on the local structure of the interface via its crystallographic orientation and components of curvature [36-43].

Growth usually also depends on the local supersaturation or undercooling, but in this limit of slow growth, changes in gradients in temperature and composition are assumed to have a negligible effect on v . The matrix can be taken to be uniformly undercooled or supersaturated, and then growth is a function only of the local geometry and can therefore be cast in terms of a geometric model. It is also possible for crystal growth to remain geometric in an imposed temperature field and to have the velocity depend on the local temperature, provided that the local temperature is not affected by the growth (examples are presented elsewhere [2]). The classical problem of crystal growth by diffusion of heat or mass is not geometric, because the velocity depends on the normal component of the gradients of temperature or concentration at the surface, and diffusion changes those gradients. However, there are geometric "toy" problems designed to capture some features of dendritic crystal growth, that do not depend on diffusion fields [46, 47]. In the screw-dislocation-catalyzed crystal growth problem, one cannot make the velocity depend on dislocation density. One must either assume that dislocations

are there in the density range where their density can effectively be ignored [45] or—with a different growth law, two-dimensional nucleation of new layers [48–50]—that they are not there at all.

In the chemical etching of an inhomogeneous microstructure, the situation can be well modelled as a geometric problem, even if v depends on the position of the surface relative to the structure being etched and on the local orientation of the surface, but not if the composition of the etchant changes significantly near the surface as a result of the etching process and this change slows the rate of etching. In ion beam etching, the erosion depends on the orientation of the surface relative to the beam and is thus geometric if there is no initial undercutting and one can ignore the effects of back-scattering [51, 52, 53]. In cellular precipitation and discontinuous coarsening [54], grain boundaries sweep through a microstructure with velocities that depend on orientation, curvature, and local structure, but not on any factors away from the boundary. In grain or domain growth, the rate of interface motion is directly related to the reduction in interfacial energy resulting from the motion and is thus geometric [53–60]. The process may depend on orientation because both the interfacial mobility and energy may depend on orientation. In the coherency-stress-driven liquid film migration [62–64], v depends on orientation of the liquid film relative to the two abutting solids and their surface compositions. It is controlled by diffusion through the liquid film, but the rate is independent of the range of the diffusion into the solid. Liquid film migration is an example where a diffusion problem can be recast as a geometric problem if the diffusion distance, which is the film thickness, remains constant. In diffusion-induced grain boundary motion in a thin foil, the problem becomes two-dimensional and geometric provided that the foil is thin enough that diffusion gradients normal to the foil can be neglected [62]. Similarly, if we ignore the effect of the stress field of the moving dislocation on itself, dislocation glide motion on a slip plane will be geometric because it is governed by local orientation and curvature and the local imposed stress field [65–67]. This is so even if a dislocation encounters obstacles to motion, for example, when the slip plane is inhomogeneous, as in a precipitation hardened structure [68–70].

In problems where there are more than two grains or phases, junctions of moving surfaces can occur. The motion of these junctions creates special problems that are only now being examined for geometrical problems [15, 17]. Multiphase or multi-grain junctions occur in grain growth and in phase transformations, such as eutectoids, in which there are more than two phases [17, 18]. An early study of the motion of Czochralski crystal growth [71–73] has led to empirical specifications for controlling the crystal-melt-vapor trijunction motion to ensure crystals of uniform diameter.

In evaluating equation (1) we have taken the Ω to be positive when there is a bulk free energy decrease for motion of the surface in direction \mathbf{n} . If we have one fluid growing into another fluid, with the normal in the direction of growth, then Ω is the same as the ΔP of Gibbs [74]. Note that Ω will be positive and wmc will be negative for a convex crystal growing into an undercooled melt, because the total surface free energy is increasing and the bulk free energy is decreasing.

Associated to a given function on unit vectors, whether it be the surface free energy per unit area γ or the mobility M , is a convex set which we call the *Wulff shape* for that function, and which we will denote by W_∞ if it is obtained from M and by W if it is obtained from γ

$$W = \{\mathbf{x} : \mathbf{x} \cdot \mathbf{n} \leq \gamma(\mathbf{n}) \text{ for every unit vector } \mathbf{n}\}$$

and

$$W_\infty = \{\mathbf{x} : \mathbf{x} \cdot \mathbf{n} \leq M(\mathbf{n}) \text{ for every unit vector } \mathbf{n}\}.$$

(If M depends on \mathbf{x} and t , then we would have a W_∞ for each \mathbf{x} and t .) It is a theorem that W is the equilibrium single crystal shape, in that it has the least surface energy for the volume it contains [38, 75, 76], and that when M is independent of everything but \mathbf{n} , W_∞ is the limiting growth shape [2, 11, 43] (and the shape that grows most slowly among all crystals of the same volume, when that volume is large enough that surface energy effects can be ignored).

For any function defined in unit vectors \mathbf{n} (and perhaps other variables), we will often extend its definition to all vectors $\mathbf{p} = r\mathbf{n}$ ($r \geq 0$) by requiring positive homogeneity of degree one. That is, we will define

$$\gamma(r\mathbf{n}) = r\gamma(\mathbf{n})$$

and

$$M(r\mathbf{n}) = rM(\mathbf{n})$$

for $r \geq 0$.

We note here that there are many other relationships between γ and W (and equivalently, in this paragraph, between M and W_∞) [77–80]. For example, when γ is a *convex function*, it is a *norm* and has a *dual norm*, and W is the *unit ball* of that dual norm. Also, when γ is differentiable as well as convex, the vector $\nabla\gamma(\mathbf{n})$ is the point on the boundary of W with exterior unit normal \mathbf{n} (and conversely). When γ is not differentiable but is still convex, then every vector in the *subgradient* of γ at \mathbf{n} is a point on the boundary of W with normal \mathbf{n} and conversely. When γ is non-convex, the plot of all the points which are $\nabla\gamma(\mathbf{n})$ or in the subgradient of γ at \mathbf{n} for some \mathbf{n} , contains W and additionally perhaps “ears” at edges or corners of W [80]. For example, see W_∞ with its additional “ears” in Fig. 1(a) of Section 4 for the *anisotropic* M of that section. Nonconvexity

of the mobility function M , and resulting “ears” on W_∞ , are possible and significant for growth problem; nonconvexity of γ tends to be less significant because of the possibility of having *varifold*, or infinitesimally corrugated, surfaces.

The formulations of surface motion problems lead to partial differential equations (PDEs) or, when W is a polyhedron and the surface is composed of plane segments, to systems of ordinary differential equations (ODEs) that are directly related to the physical growth law. The solutions to these equations track the position of the surface. Methods for treating geometric crystal growth can be divided roughly into two groups, direct ones where the motion of the interface is explicitly considered, and indirect ones where the interface at each time is the *level set* of a function defined on space-time and is only moved implicitly by the dependence of the whole function on time. In the indirect cases, the functions sometimes have an artificial quality, except on the crystal surface, but in spite of this apparent complication, these methods often have advantages in terms of characterizing the solutions independent of parametrization. In the special case where the normal velocity does not depend on the curvatures of the surface, the function can (but need not) be given the meaning of time less the “arrival time” of the crystal at a point, altering the problem to finding level sets of the arrival time. (As will be noted in Section 2.4, the arrival time is not always that of the minimum-time path when non-convex velocity functions are used, but that is immaterial here.) For some indirect methods, the formulation is modified, so that unphysical factors are brought in to facilitate the computation or theory; for these, it must be shown that the solutions converge to those of the correct geometric problem. Computer programs have been written to implement many of these methods, both direct and indirect. All of these methods are intended to solve the same types of surface motion problems and where applicable should give the same results. However, there are certain conditions for the application of each method. Some are valid only if v is not dependent on curvature, for then the PDE is first order. Some are valid if the dependence of v on \mathbf{n} and/or its derivatives satisfy certain continuity conditions, such as that the function be C^2 (see Glossary). Some methods are only valid for a single crystal embedded in a matrix; others can deal with more than two phases and junctions of surfaces. Whether or not M or γ are *convex functions* can be important. It should be noted that no nucleation is allowed in these problems: all deal only with the motion of pre-existing interfaces.

In order to understand the indirect methods, consider u to be a real-valued function of space and time that takes on a particular value (such as zero) along the crystal surface at each time. The motion of the surface is then tracked by following the motion of a “level set” (e.g. the zero set) of u . If u is any

differentiable function of \mathbf{x} and t , then for fixed \mathbf{x} and t and small $\Delta\mathbf{x}$ and Δt ,

$$u(\mathbf{x} + \Delta\mathbf{x}, t + \Delta t) \cong u(\mathbf{x}, t) + \nabla u \cdot \Delta\mathbf{x} + u_t \Delta t.$$

Here ∇u is the spatial gradient of u , i.e. $\nabla u = (\partial u / \partial x_1, \partial u / \partial x_2, \partial u / \partial x_3)$, and $u_t = \partial u / \partial t$. If \mathbf{x} is on the level set of u at time t [e.g. $u(\mathbf{x}, t) = 0$] and $\mathbf{x} + \Delta\mathbf{x}$ is on the level set at time $t + \Delta t$, then $u(\mathbf{x} + \Delta\mathbf{x}, t + \Delta t) = u(\mathbf{x}, t)$, and so

$$\frac{-\nabla u \cdot \Delta\mathbf{x}}{\Delta t} \cong u_t.$$

Now $\pm \nabla u$ is automatically normal to level sets of u , so if we take $\Delta\mathbf{x}$ to be a multiple U of $-\nabla u / |\nabla u|$, then the limit V of $U / \Delta t$ as Δt goes to zero is the normal velocity of the level set, measured relative to the direction of decreasing u , for this particular u , \mathbf{x} , and t . Thus we have

$$v = u_t / |\nabla u|.$$

This is always true, for any u , since it is just a geometric statement. If the normal velocity is specified for physical reasons, we can substitute that velocity for V (assuming that we choose the initial values of u so that the normal vector \mathbf{n} is in the direction of decreasing u , so $\mathbf{n} = -\nabla u / |\nabla u|$) and obtain a partial differential equation for u . That is, if we are given a normal velocity as a function v of position \mathbf{x} , time t , and normal direction \mathbf{n} , a PDE in which every level set moves by that normal velocity is

$$\partial u / \partial t - |\nabla u| v(\mathbf{x}, t, -\nabla u / |\nabla u|) = 0.$$

Such an equation is a Hamilton–Jacobi equation [5]. When curvature is included, the PDE is a second order non-linear equation of the form

$$\partial u / \partial t - |\nabla u| v(\mathbf{x}, t, -\nabla u / |\nabla u|, \nabla(-\nabla u)) = 0$$

where v depends on the derivatives of $\nabla u / |\nabla u|$ only in the directions perpendicular to $\nabla u / |\nabla u|$. Since $\text{div}(-\nabla u / |\nabla u|)$ (the divergence of the normal vector) is the mean curvature of the level surface, motion by mean curvature is an example which can be put into this context, as

$$\partial u / \partial t = -|\nabla u| \text{div}(-\nabla u / |\nabla u|).$$

There are, in addition, two formulations that are not geometric, but their solutions approximate in some sense the solutions to a geometric problem. In the phase field method described in the next section, the PDE describes a function in all space that is supposed to have physical significance, namely the extent to which that part of space is in one particular phase; in certain limits, the motion of level surfaces of its solution reduces to a geometric problem. Order–disorder transformation problems and Monte Carlo simulations of a Q-state Potts model on a lattice give rise to surface formation and motions that also appear to mimic those of geometric problems, but exactly what continuous model this

discrete model approximates is far from known at this point.

In the next section we will summarize these two methods which are not strictly geometric as well as the seven that are formulated as geometric methods. We will examine the advantages of each method, when it is applicable, and when methods are equivalent. It will be seen that no method is applicable for all the problems that can be solved.

In the third section, several methods (crystalline, characteristics, level sets) will be described in greater detail, and in the fourth section simple examples will be used to illustrate the methods. In the fifth section, various computational schemes will be surveyed. In the discussion section, a variety of open problems are collected. A glossary of mathematical terms is presented in an appendix. In the paper following this one, we summarize all the various forms in which the mean curvature or weighted mean curvature is written, and indicate why they are mathematically equivalent (although not equally useful in all situations).

2. SUMMARY OF NINE METHODS FOR GEOMETRIC CRYSTAL GROWTH

Nine methods are described briefly below for doing motion of surfaces where the normal velocity is given by

$$v = M(\mathbf{n}) [\Omega(\mathbf{x}, t) + wmc]$$

where M and Ω are given functions. All of the direct methods being given before all of the indirect methods, and the order otherwise is approximately historical. For each of them, the least restrictive conditions that the mathematics requires are usually given, even though there might not be any physical situation which naturally imposes those conditions.

2.1. The nine methods

2.1.1. Mapping of a fixed manifold (like a circle or line in the plane or a sphere or plane in 3-space) (direct). The direct formulation is to solve for the family of mappings \mathbf{f}_i (parametrizations) such that

$$(d/dt)\mathbf{f}_i(\mathbf{p}) = \mathbf{n}M(\mathbf{n}) [\Omega + (a_1 \kappa_1 + a_2 \kappa_2)],$$

where κ_1 and κ_2 are the principal curvatures of the surface at $\mathbf{x} = \mathbf{f}_i(\mathbf{p})$ (the curvatures are taken to be negative for a convex body oriented so that its normal vector points outward) and $a_i = \partial^2/\partial p_i^2 \gamma$, where p_i is the variable in the direction of the i th principal curvature and γ is assumed to have been defined on all vectors (otherwise, differentiation with respect to spherical coordinates produces extra terms; see the companion paper [34]).

This is the classical approach for motion by mean curvature, adopted by many including Mullins [57, 58], Gage and Hamilton [81], Gage [82, 83], Grayson [84], Huisken [85, 86], Ecker [87, 88], Hass and Scott [89], Angenent [90, 91], and Gurtin [13]

(although Angenent and Gurtin rotate everything by 90 degrees, and use the inward-pointing rather than exterior normal). Short time existence in this mapping formulation follows from the work of Ladyzhenskaya [92]. This approach should also be amenable to the case where v does not depend linearly on driving force (which is equivalent to an M that depends on v), although little attention has been directed to that case. Also several computational models are built on this idea, including those of Brakke [93], Dziuk [94], etc. For curves in 2-d, Frost [95] has done extensive simulation of grain growth.

Problems with the mapping approach include the difficulty of handling topological changes (e.g. a dumbbell pinching off at its neck, or a crystal shrinking to zero size), in particular due to the formation of singularities in the flow [97]. A philosophical problem is the fact that something "non-canonical" has been introduced by the parametrization which is inherent in the mapping approach; the solution to geometric motion depends only on the shape and not on how the shape is parametrized. Also there is a question about what to do at corners and edges in the initial surface, which are places where neither the normal nor both curvatures are defined, so that the motion law above cannot be directly applied. In this case, there are often a number of possible surface evolutions that obey the given motion law on their *smooth* parts; one of these possibilities is often some obvious type of extension of the smooth parts until they meet. For example, if one has *isotropic* and curvature-independent normal growth ($M \equiv 1$, $\gamma \equiv 0$), an initial cube might be thought to grow by simple expansion of the cube. However, this type of growth is not stable, in that a slight smoothing of the corner, or even introduction of one additional facet, would result in dramatically different growth. Similar problems can arise in decisions of how to handle γ and M that are not C^2 or are nonconvex. We apply in this paper the physical criterion that the growth should be stable under continuous perturbations; the reasons for making any other choice ought to be explicitly delineated. Which criteria are physically reasonable is a question that needs experimental investigation.

2.1.2. Brakke's formulation [3] (direct, sort of). Brakke, in a very important but difficult early paper, developed a theory of motion of *varifolds* by mean curvature that is a weak formulation in terms of smooth test functions. One observes that if S_t is a family of smooth surfaces moving by any velocity v , and if ϕ is a smooth non-negative function which is nonzero on a closed and bounded region in R^3 , then

$$\frac{d}{dt} \int_{S_t} \phi \, d\sigma = \int_{S_t} v \cdot \nabla \phi \, d\sigma - \int_{S_t} \phi v \cdot h \, d\sigma$$

(here $d\sigma$ refers to integration with respect to surface measure). Therefore, Brakke defines a family of varifolds S_t , with associated measures $\|S_t\|$ and mean

curvature vector fields h as defined by Allard [98], to be moving by their mean curvature if for each such smooth test function ϕ

$$\frac{d}{dt} \int \phi \, d\|S_t\| = \int h \cdot \nabla \phi \, d\|S_t\| - \int \phi h \cdot h \, d\|S_t\|$$

whenever the mean curvature vector field h has

$$\int h \cdot h \, d\|S_t\|$$

finite (and is $-\infty$ when it is not finite). This context allows the presence of triple junctions, point junctions, and the like as part of the general varifold definition. Brakke proved general existence results in this context, by a complicated process involving time steps going to zero and two different types of motions per step, but he obtained only partial regularity results and no one else has been able to improve them; there is also no uniqueness in this framework.

When the initial surface is smooth and without self-intersections, Brakke showed that for some interval of time, the motion is unique and the surface stays smooth without intersection. Under these conditions the method solves the classical direct formulation.

The method works well for more than two phases, accomplishing topological changes when needed. It assumes the surface energy is the same on all interfaces and has no additional driving force Ω due to phase change.

Several people are currently studying Brakke's paper, trying to relate other approaches to his approach and to prove more about the behavior of his motion.

2.1.3. "Crystalline" method [12, 16–19] (direct). The *crystalline* method works if the surface free energy γ and the mobility M are each given on the same finite set of unit vectors, essentially those which become the normals of the Wulff shape W for the surface energy, and with the value of M on all other directions being determined by its values on these directions via $M(a\mathbf{n}_1 + b\mathbf{n}_2 + c\mathbf{n}_3) = aM(\mathbf{n}_1) + bM(\mathbf{n}_2) + cM(\mathbf{n}_3)$ if facets with orientations \mathbf{n}_1 , \mathbf{n}_2 , and \mathbf{n}_3 meet at a corner of W and a , b and c are non-negative numbers. The fact that the given set of unit vectors are to be the normals of W implies that the values of γ on all other directions are at least those determined by its values on the given finite set, so that $\gamma(a\mathbf{n}_1 + b\mathbf{n}_2 + c\mathbf{n}_3) \geq a\gamma(\mathbf{n}_1) + b\gamma(\mathbf{n}_2) + c\gamma(\mathbf{n}_3)$ under the same conditions as above.

This method converts the PDE problem into a system of ordinary differential equations (ODEs) for the distances of the plane segments from some fixed origin

$$ds_i/dt = M(\mathbf{n}_i) [\Omega + wmc(i)]$$

where $wmc(i)$ stands for the weighted mean curvature for the i th plane segment in this crystalline context (it is defined in Section 3.2 and explained and related

to the other expressions for wmc in the following paper [34]). These equations can be solved numerically (and sometimes analytically). The method can handle fixed boundaries and multiple grains or phases (with the same or different surface energies and mobilities for different types of interfaces). Like the mapping approach, this method should be applicable to the case where v does not depend linearly on driving force, although no results have been published in that case. Both theory and computer programs have been fairly extensively developed in the 2-dimensional case; the full three dimensional case is only partially investigated and programmed at this point. The extent to which the motion for an arbitrary γ and M can be approximated by this type of polyhedral motion is also currently under investigation. In fact, Roberts [96] developed the same method, in the case of simple closed curves, purely for the purpose of approximating motion of curves by curvature. The method does use a type of parametrization of the surface, but one that is natural in that it just lists the normals and distances of the facets together with their adjacencies.

2.1.4. Least time method [15, 99, 100] (indirect). If $\gamma \equiv 0$ and M is a convex function of the normal direction \mathbf{n} , and if it and Ω are constant or *Lipschitz* functions of \mathbf{x} and t , then the time τ at which the interface reaches \mathbf{x} is the minimum time of travel over all *rectifiable paths* (see glossary) from the initial crystal interface to \mathbf{x} , where the time to travel along a path is the integral of $1/|Vv[\mathbf{n}(\mathbf{x})]|$ along the path, $\mathbf{n}(\mathbf{x})$ being chosen so that $Vv[\mathbf{n}(\mathbf{x})]$ is in the direction of the tangent to the path at \mathbf{x} . It gives the same results for convex M as the method of characteristics when there are only two phases, since a characteristic is a minimum time path, except that it applies additionally to surfaces which are not *piecewise* C^2 . This formulation of the problem is also applicable for more than two phases (which means there are three or more types of surfaces, with different velocity functions, which can meet along multiple-junction curves or points), giving unique evolutions of the various interfaces under physically realistic assumptions on the different velocity functions and for most initial data [15]. To work with non-convex mobility and single interfaces, one must go to a game-theory type minimax problem for the time [99] instead of just minimizing time over all paths. The minimax characterization is not unique, but this one seems appropriate since it gives the viscosity solution (described in Section 7 below) and the viscosity solution satisfies the type of stability described at the end of method (1) above.

No minimax time formulation has been made for non-convex velocity functions where there are more than two phases, and no minimum or minimax time formulation can be made with a velocity that depends on curvature. But within its scope, the minimum time approach does provide proofs of existence and uniqueness of solutions, and it does enable one to

verify whether particular evolutions satisfy the given growth law.

2.1.5. *Method of characteristics* [2, 40–42, 101, 102] (*indirect*). This method applies when the normal growth rate v is a given function of position \mathbf{x} , time t and exterior unit normal \mathbf{n} but not a function of curvature. We thus take $\gamma \equiv 0$ and $v(\mathbf{x}, t, \mathbf{n}) = \Omega(\mathbf{x}, t)M(\mathbf{x}, t, \mathbf{n})$. The general implicit PDE is then the first order equation

$$\partial u / \partial t - |\nabla u|v(\mathbf{x}, t, -\nabla u / |\nabla u|) = 0.$$

As before, it is convenient to extend M (and thereby v) to be a function on all vectors so that $v(\mathbf{x}, t, r\mathbf{n}) = rv(\mathbf{x}, t, \mathbf{n})$ for all $r > 0$. The equation then simplifies to

$$\partial u / \partial t - v(\mathbf{x}, t, -\nabla u) = 0.$$

We can give u a physical meaning if we assume $u(\mathbf{x}, t)$ can be written as $t - \tau(\mathbf{x})$ when v is positive and as $\tau(\mathbf{x}) - t$ when v is negative; $\tau(\mathbf{x})$ is thus the arrival time of the crystal surface at the point \mathbf{x} . Here the exterior normal \mathbf{n} of the crystal surface is $\pm \nabla \tau / |\nabla \tau|$, a unit normal in the direction of increasing τ for growth of that crystal and in the opposite direction for its dissolution. The general implicit equation then becomes the non-linear, first-order PDE

$$v(\mathbf{x}, \tau, \nabla \tau) = 1$$

when v is positive, and when v is negative it becomes

$$v(\mathbf{x}, \tau, -\nabla \tau) = -1$$

or equivalently

$$\hat{v}(\mathbf{x}, \tau, \nabla \tau) = 1,$$

where $\hat{v}(\mathbf{x}, t, \mathbf{p}) = -v(\mathbf{x}, t, -\mathbf{p})$. (Note that in order to use this arrival-time reformulation of the problem, special attention has to be paid to places where $v = 0$.)

First order PDEs can often be solved by the method of characteristics (see 3.1 below). This method can accommodate discontinuities in the slope, i.e. corners and edges, whose appearance results from *shocks*, and the rounding of corners and edges with the appearance of a range of new orientations, through the use of *fans* of characteristics. The method works for a velocity v which is a *piecewise* C^2 function of normal direction and otherwise is either constant or is a C^2 function of position \mathbf{x} and time t . (In particular, v is not allowed to depend on any curvatures.) The method of characteristics is useful primarily for simple initial shapes and for computing solutions by hand; many features of crystal growth with such a given velocity can be understood by this method.

2.1.6. *Regularization, by addition of smoothing (non-physical) term to equation (implicit)*. Examples are adding ε times the Laplacian Δu of u for first order PDE or fourth order elliptic term to second order PDE [103]. Consequences of adding a fourth

order elliptic term have not yet been investigated; in particular it is not known whether it converges to what we want for nonconvex M and nonzero γ .

2.1.7. *Viscosity solutions* [1, 4–9, 11, 104–109] (*indirect*). As stated previously, one would like to look at level sets of the PDE

$$u_t - |\nabla u|v(t, -\nabla u / |\nabla u|, \nabla(|\nabla u| / |\nabla u|)) = 0$$

where the dependence on $\nabla(|\nabla u| / |\nabla u|)$ satisfies certain conditions. Problems occur when $\nabla u = 0$ or u is not C^2 (one cannot take second derivatives of a function that is not C^2), so that this equation must be interpreted in some weak sense when singularities might develop or be present initially in the interface. There are various definitions of weak solutions for different types of PDE. A viscosity solution of the PDE for geometric crystal growth is a particular type of weak solution that embodies the principle of barriers; one in effect sandwiches the surface between smooth surfaces whose behavior one can compute with the original PDE. The function u here has no particular physical meaning and its only purpose is to define the crystal surface at each time t ; the crystal surface at time t is the level set consisting of the points \mathbf{x} where $u(\mathbf{x}, t) = 0$ (a “contour line” on the graph of u as a function of \mathbf{x} at a particular time t). One might want to make u be $t - \tau(\mathbf{x})$ as before, but there are several reasons not to require this, the most important being that almost certainly such a u would not satisfy the PDE for (\mathbf{x}, t) such that $u(\mathbf{x}, t) \neq 0$. Also, the answer for all time would be incorporated in the values of the function u at $t = 0$, in that the crystal surface at time T would be the level set $u(\mathbf{x}, 0) = T$, so that one would need to know the solution for all time as part of the initial data. Finally, it is difficult to allow for τ to be “multiple-valued” when the interface passes back and forth through a point several times, as will often happen.

If v depends on weighted mean curvature, then the surface energy function γ must be C^2 and convex. At our present state of knowledge any dependencies on position \mathbf{x} must be continuous, but this might be an artefact of the current state of the theory. Under hypotheses to be discussed in a later section, there is one and only one viscosity solution for any continuous initial data, even for u whose level sets have corners and edges. Because of this, the method is useful for constructing mathematical proofs about various properties of the motion for initial values of u such that level sets have corners and edges. It is also useful for computer calculations, even in the case where we take $\gamma \equiv 0$, as it is often easier to handle topological changes by determining level sets of a function than by tracking characteristics and trying to find and follow shocks. The cost is that one must calculate u on all of space-time when one is only interested in the set where u is zero. However, the solution is not reasonable physically when there are more than two phases, or in situations where physically correct notions of motion by mean curvature do

not depend continuously on the initial data, such as is the case in Fig. 5 of Section 4. In all these situations, the viscosity solutions seem to “develop an interior” [99]. This means that the set on which $u = 0$ at time t is not just a “contour line” (or surface) but expands to fill a whole two-dimensional region in the plane (or 3-dimensional region in 3-space); see Fig. 5(e) in Section 4. Some type of vector-valued function u is probably needed in the multiple-phase case, but such a theory has not yet been developed. Osher [110], working with Bence, has begun to explore computationally the use of a vector-valued u , and preliminary results are comparable to those of Taylor [15]. When $\Omega = 0$ and there are only two phases, the level set approach gives the same solutions as the least time (or minimax time) approach [99]. It appears that this method cannot be extended to apply to the case where the dependence of v on driving force is not linear.

2.1.8. Phase field methods [21–28, 35, 36] (indirect). Here the interface is defined by a level set of a solution to the PDE

$$u_t = \varepsilon \Delta u + (1/\varepsilon) f(u)$$

where f is the derivative of a double-well potential, Δu denotes the Laplacian of u in the \mathbf{x} coordinates, and u is an “order parameter” that is used to track the position of the interface (the narrow region where u changes from its value at one of the wells to its value at the other well). This type of equation, called a reaction-diffusion equation, does not fit the geometric hypotheses for the type of PDE considered here. However, when the curvatures of the level surfaces are small, solutions to this equation are approximately solutions to the equation of the preceding method

$$u_t = |\nabla u| [C + \varepsilon \operatorname{div}(\nabla u / |\nabla u|)]$$

where C is related to the difference in depths of the wells. Such results were found by Cahn and Allen for the first equation with equal depth wells, and this equation has been investigated fairly extensively [36, 37]. A related equation is the Cahn–Hilliard equation

$$u_t = \Delta [f(u) + \Delta u]$$

which has conservation of u (since $\int u_t = 0$ if the boundary of the region can be ignored). As stated, the reaction diffusion equation applies only to isotropic motion including a mean curvature component, although anisotropic analogues have been constructed by letting ε depend on $\nabla u / |\nabla u|$. Rubenstein and coworkers [23, 24] did formal asymptotics to show convergence to motion by mean curvature. Bronsard and Kohn [21, 22] proved convergence rigorously in the radially symmetric case. Recently Evans, Soner and Souganidis [111] have shown rigorously that the limits of the phase field solution as ε goes to zero is the same as the viscosity solution of the indirect formulation, when $\Omega = 0$ and γ and M are

isotropic and when the viscosity solution does not develop an interior. In order to apply the phase field method to situations with more than two phases, it would be necessary to introduce more order parameters. For a description of the phase field approach including diffusion of heat and all of its limits, see the survey paper of Caginalp [28]. This method looks very promising for computation when diffusion fields must be included [112], but there are pitfalls that must be recognized, including numerical ones mentioned by Osher [110] and analytical ones, such as that the *ad hoc* way of introducing anisotropy by making ε be a function of ∇u changes the order of the equation.

2.1.9. Order-disorder transformations and Monte Carlo simulations via a Q -state Potts model on a lattice [59, 60, 113–119]. This method is most like a direct method but since it deals with a lattice of points, there is actually no surface and no normal direction and no curvature.

Initially a “state variable”, which is an integer q between 1 and Q , is assigned to each point in a lattice. The energy of a lattice site is usually taken to be the total number of nearest neighbor pairs with differing states; sometimes the energy is taken as a weighted sum, depending on the states of the site and its neighbors, and sometimes second nearest neighbors as well as nearest neighbors are considered. All points with the same state variable q can be thought of as being crystalline regions with the same structure, so that a “grain” is a region where all the lattice points have the same value of q .

At each time step, one picks a point of the lattice at random and a state, and has the point change to that state with a probability of 1 if the energy remains the same or decreases (due to the effect of the neighbors), and with a probability that depends on the temperature (and is zero if the temperature is at absolute zero) if the energy is increased. Volume conservation can be imposed by picking pairs of points and interchanging their types if it is not disadvantageous energetically, although this takes one even further from the realm of geometric motion.

Either as part of the initial configuration, or as a result of the very early stages of the simulation, points of the same type cluster into a number of regions. The interfaces are then defined to be the boundaries between those regions. (One could make this precise by assigning to each point its closed Voronoi cell—the region which is closer to that lattice point than to any other lattice point—and then taking the union of all the Voronoi cells whose centers have state q as being the region of state q , and consider the interfaces to be the union of all the boundaries of the regions; however, the local structure of those boundaries determined by the cell shapes is not really relevant.)

“Steps” on these boundaries can be considered to be at lattice points that can change from one state

to another with no net energy change. (In 3-d, this is better described as a kink on a step.) At absolute zero temperature, all changes occur only at the boundaries, and the motion is a random walk of “steps” limited to be between adjacent “steps,” together with the irreversible energy-decreasing change of a point from one state to another, when an “up” step annihilates a “down” step or a “step” disappears at a triple junction, perhaps with the creation of a new “step”.

It is not at all clear what continuous model this discrete model approximates. It is a stochastic motion whereas the rest of this paper is about deterministic models. The model does reduce energy monotonically, and the energy is associated with the boundaries. In fact, a standard way to compute surface energy in crystals is by counting bonds cut to make a surface, and since the Potts model is a bond-counting model, there is a specific surface energy γ associated with it, and the energy of the Potts model lattice is the total surface energy. At absolute zero temperature, one can compute that the Wulff shape associated with γ is a polygon in 2-d (a polyhedron in 3-d), and γ is convex. For example, the Wulff shape for a 2-d triangular lattice is a hexagon, if one looks only at nearest neighbors in determining the energy, or a regular dodecagon, if one assigns the same energy to first and second nearest neighbors. However, it seems far beyond either the theory or the experimental evidence to conclude that the motion is motion by mean or weighted mean curvature. The most one can say seems to be that in 2-d when $Q = 2$, the area of a region of one type surrounded by a region of the other type has been observed to decrease linearly with time, and for large Q , the energy, which is a measure of the length of the boundaries, is observed to vary with the negative one-half power of t after an initial transient and until the grain size approaches the computational grid size. Also, for nearly zero slopes where all steps are of the

same type (up or down), if the random walk of steps gives a density of steps which satisfies the diffusion equation [114] then the motion is approximately motion by curvature since the integral of the diffusion equation is approximately the motion by curvature equation (since the density of steps gives the slope of the interface).

2.2. Relationships, in the two phase case (in particular, no triple junctions)

The relationships among methods discussed in this and the following section are summarized in Table 1.

When $\gamma \equiv 0$ and the solutions are smooth surfaces, methods (1) (classical mapping), (4) (least time), (5) (characteristics), (6) (regularization) and (7) (level set) are applicable and all are equivalent. (See Lions [103] for the equivalence of (6) and (7) with (4).) Note, however, that non-smooth solutions (i.e. surfaces with corners and edges) can quickly develop, even with smooth initial surface.

When $\gamma \equiv 0$, M is convex, and solutions are not smooth, methods (4–7) are applicable and equivalent (again, see Lions [103]). In the 2-d case where W_∞ is a polygon and the initial surface is polygonal with each facet parallel to a face of W_∞ , then (3) (crystalline) also applies and is equivalent to these; the 3-d case has not been investigated. When $\gamma \equiv 0$ and M is non-convex, methods (4), (6) and (7) are applicable and equivalent, although one has to use the minimax approach in place of least time in (4) [99]. When one can tell which characteristics to use, (5) is also applicable and equivalent ([2], [4] and [5]). Again, in the 2-d case where the solutions ought to be polygonal, method (3) applies.

When $\Omega \equiv 0$, M and γ are isotropic, and solutions are smooth surfaces, methods (1), (2) (Brakke’s varifold), (7) and (8) (phase field) are applicable and equivalent. (9) is often used, but it actually introduces some anisotropy due to the lattice, and its behavior

Table 1. Theory

Method	Initial surface	γ (n)	M (n)	Ω (x, t)	Multiple grains?	Topological changes?
Mapping						
—standard	Smooth	$C^{4,\alpha}$ and strictly convex	$C^{2,\alpha}$	$C^{2,\alpha}$	No	Difficult
—Angenent	Smooth, curves ^a	$C^{2,1}$	Lip.	Ind. of x Lip. in t	No	Difficult
Brakke’s varifold	Rectifiable varifold	Isotropic	Isotropic	$\equiv 0$	Yes	Automatic
Crystalline	Faceted, curves ^d	Crystalline	Any compatible with γ	c^d	Yes	Easy
Least time	Rectifiable	$\equiv 0$	Convex	c^d	Yes	Automatic ^b
Characteristics	Piecewise C^2	$\equiv 0$	Piecewise $C^{2,c}$	Piecewise C^2	Yes	Difficult to find and track shocks
Regularization	C^2	$\equiv 0$	C^0	C^0	No	Automatic
Viscosity	C^0	C^2 and strictly convex	C^0	C^0	No	Automatic
Phase field	C^2	Isotropic ^d	Isotropic ^d	c	No	Automatic
Q -state Potts	Anything on lattice	Relevance unclear	Isotropic	$\equiv 0$	Yes	Automatic

Note: C^0 is continuous; “c” is constant; “Lip” is Lipschitz. $C^{n,\alpha}$ refers to a type of differentiability (Holder) that is stronger than C^n but weaker than C^{n+1} .

^aCan handle some corners compatible with γ .

^bAutomatic only because of definition of least time method.

^cIncomplete results for nonconvex M .

^dBelieve that these restrictions are not essential to the method.

is less understood theoretically. When $\Omega \equiv 0$, M and γ are isotropic, and solutions are not always smooth surfaces, methods (2), (7) and (8) are applicable. There are serious questions here about whether the solutions of (7) can develop an interior. When they do not do so, then (7) and (8) are equivalent [111]. When they do, it is strongly suspected that the solutions of (2) are non-unique. Again (9) is used. When $\Omega \neq 0$ and M and γ are anisotropic and solutions are smooth surfaces, then methods (1) and (7) are applicable and equivalent.

When $\Omega \neq 0$, M and γ are anisotropic, and solutions are *not* known to be always smooth surfaces, then method (7) is applicable when γ is C^2 and *strictly convex*, and method (3) is applicable when W is a polyhedron (again, the method is primarily 2-d at this point; the 3-d case is only partly worked out). It is strongly suspected that these two methods can be used to approximate each other in some way. Method (1) has been extended to work for limited times [12]. In method (9), an anisotropy in γ leading to polyhedral W occurs at zero temperature, but the motion obtained is almost certainly not motion by the appropriate weighted mean curvature.

2.3. Relationships, three or more phases or grains

When $\gamma \equiv 0$ and M is convex, methods (4) and (5) are applicable and equivalent (with the proper interpretations). Method (3) is applicable (in 2-d, at least) if W_∞ is polyhedral and the initial surface is polyhedral.

When $\Omega \equiv 0$ and M and γ are isotropic, only (2) really applies. Method (9) has been used, primarily in 2-d (though some 3-d computations have been made), although again it introduces some anisotropies and is not well understood theoretically. Several computer schemes based on method (1) in 2-d [93, 95] and 3-d [93] exist, but there is at present little theory to accompany them.

In 2-d, when W is a polygon and the initial curves are polygonal, method (3) is applicable (theoretically and computationally), though whether the variational formulation used is "correct" might be debatable, and solutions have not been shown to be unique.

3. ELABORATIONS ON THREE OF THE METHODS

3.1. The method of characteristics

The method of characteristics applies when the normal velocity of the surface is given as a *piecewise* C^2 function v of position \mathbf{x} , time t , and unit normal direction \mathbf{n} , but not of any curvatures. This method is indirect; the surface at time t is the set of points \mathbf{x} such that $u(\mathbf{x}, t) = 0$ (i.e. the zero-level set), where u satisfies the PDE

$$\partial u / \partial t = |\nabla u| v(\mathbf{x}, t, -\nabla u / |\nabla u|).$$

We again extend v by *positive homogeneity of degree one* to be a function on all vectors \mathbf{p} rather than just unit vectors \mathbf{n} , so that the equation becomes

$$\partial u / \partial t - v(\mathbf{x}, t, -\nabla u) = 0.$$

As noted in Section 2, if one can set $u = \pm[t - \tau(\mathbf{x})]$, then τ is the arrival time of the surface at \mathbf{x} (the time at which the surface passes through the point \mathbf{x}). We choose the sign so that the oriented unit normal to the crystal surface is in the direction $-\nabla u$, and thus choose it to be the sign of v . It is possible to define this time τ uniquely if v is always of one sign, and often to define it locally for short intervals of time even if v changes sign. Note that $\nabla \tau(\mathbf{x}) / |\nabla \tau(\mathbf{x})|$ is the unit normal in the direction in which the crystal interface is moving and is thus $\mathbf{n}(\mathbf{x})$ (the outward unit normal of the crystal) if the crystal is growing and $-\mathbf{n}(\mathbf{x})$ if the crystal is shrinking. We can assume that v is non-negative by replacing it by $-v(\mathbf{x}, t, -\mathbf{n})$ where necessary, and the equation becomes

$$F(\mathbf{x}, \tau, \nabla \tau) \equiv v(\mathbf{x}, \tau, \nabla \tau) - 1 = 0.$$

The main advantages of this formulation over the u formulation are that it deals with a physically meaningful quantity, the arrival time, rather than the abstract quantity u , and that the characteristics track the motion of points on the surface as shown below.

The theory of first order PDE (see, for example, John [101]) asserts (under conditions of smoothness of the given function $F(\mathbf{x}, \tau, \mathbf{p})$ in all its variables and of the initial data to be specified shortly) that the initial value problem can be solved by the use of curves called *characteristics*. These curves, parametrized by some variable s and thus written as $\mathbf{x}(s)$ [and with $\tau = \tau(\mathbf{x}(s))$ and $\nabla \tau[\mathbf{x}(s)] = \mathbf{p}(s)$ at $\mathbf{x}(s)$], emanate from each point in the initial surface and are determined by the following set of seven ordinary differential equations

- (1) $dx_i/ds = \partial F / \partial p_i$ for $i = 1, 2, 3$
[i.e. $d\mathbf{x}/ds = \nabla_{\mathbf{p}} F(\mathbf{x}, \tau, \mathbf{p})$]
- (2) $d\tau/ds = \sum_i p_i \partial F / \partial p_i$ [i.e. $d\tau/ds = \mathbf{p} \cdot \nabla_{\mathbf{p}} F(\mathbf{x}, \tau, \mathbf{p})$]
- (3) $dp_i/ds = -\partial F / \partial x_i - p_i F / \partial \tau$ for each i
[i.e. $d\mathbf{p}/ds = -\nabla_{\mathbf{x}} F - \mathbf{p} \partial F / \partial \tau$].

Because $\mathbf{p} \cdot \nabla_{\mathbf{p}} F = \mathbf{p} \cdot \nabla_{\mathbf{p}} v = v(\mathbf{p}) = 1$, (2) above will always reduce to $d\tau/ds = 1$ for this crystal growth problem, and so the parameter s along the characteristics can be taken to be the arrival time τ . Note that since only derivatives of F appear in these equations, we can replace F by v in the above equations. If v does not depend explicitly on \mathbf{x} , then (3) becomes

$$(3') \quad d \ln(p_i) / ds = -\partial v / \partial \tau$$

(unless p_i is initially 0, in which case p_i stays 0 for all time on that characteristic) for each i . Since $\ln p_i$ has the same derivative for each i (or $p_i = 0$), we conclude that the ratios of the p_i are constant along

characteristics when the velocity does not depend explicitly on position, and thus that the normal $\mathbf{n} = \mathbf{p}/|\mathbf{p}|$ to the crystal stays constant along characteristics in this case (though \mathbf{p} may change in magnitude). Thus in this no-spacial-dependence case, a characteristic is the trajectory of a point with a given normal as the crystal grows. (Such is not the case when v depends on \mathbf{x} , as a temperature-gradient example demonstrates [2].)

If v does not explicitly depend on either the arrival time τ or spacial position \mathbf{x} , then (3) becomes

(3'') $d\mathbf{p}/ds = 0$, which says that \mathbf{p} as well as $\mathbf{n} = \mathbf{p}/|\mathbf{p}|$ is constant along characteristics,

and (1) becomes

(1'') $d\mathbf{x}/ds = \nabla_{\mathbf{p}}v$, which says that characteristics are straight lines of the form

$$\mathbf{x} = \mathbf{x}_0 + t\nabla v(\mathbf{n}_0)$$

for $t \geq 0$, where $\mathbf{x}(t)$ is on the surface of the crystal at time t . [Here $\nabla v(\mathbf{n}_0)$ means that we are evaluating the gradient at \mathbf{n}_0 , not that we are taking any kind of surface gradient. Note that ∇v is constant in radial directions.]

The crystal shape at time t is the locus of all the points $\mathbf{x}(t)$ on all the characteristics from initial points \mathbf{x}_0 , as long as these characteristics do not cross. When v depends only on \mathbf{n} and not \mathbf{x} or t , if we follow an element of surface of a given orientation \mathbf{n} , it will travel with constant velocity, here given by $\nabla v(\mathbf{n})$. Since the plot of $\mathbf{n}/v(\mathbf{n})$ is the level set $v(\mathbf{p}) = 1$ for the function $v(\mathbf{p})$, and since $\mathbf{p} \cdot \nabla v(\mathbf{p}) = v(\mathbf{p})$, this is equivalent to Frank's result [40], which said that the element moves in the direction \mathbf{n}' of the normal to the polar plot of the slowness vectors $\mathbf{n}/v(\mathbf{n})$ and with a speed given by $v(\mathbf{n})/(\mathbf{n} \cdot \mathbf{n}')$. The gradient of v as a function of \mathbf{p} turns out to be of central importance in this model. It is similarly of central importance (and called ξ [79, 80]) in determining equilibrium shapes of curved surfaces with anisotropic surface free energy $\gamma(\mathbf{n})$. We can apply some of the known relations between γ , its gradient, and its Wulff shape W . A summary of results relating $v(\mathbf{n}), v(\mathbf{p}), \nabla v$ and W_∞ are given in the Appendix of our earlier paper [2]. The relationship between v and W_∞ has been well-studied, especially in the case where v is a convex function (which is equivalent to that plot being convex) (see, for example, Refs [77, 78]). Cahn and Hoffman [80] rediscovered many of these results for the case when v is interpreted as a surface energy function γ . When v is a convex function, v is the support function of its W_∞ , and W_∞ is the plot of ∇v . Note that if \mathbf{x} is a boundary point of W_∞ and the plane with normal \mathbf{n} through \mathbf{x} is a *support plane* of W_∞ , then $\mathbf{x} \cdot \mathbf{n} = v(\mathbf{n})$ when v is convex. One can regard W_∞ itself as the plot of $\mathbf{n}w(\mathbf{n})$ for some function w defined on unit vectors and then extend w by $w(r\mathbf{n}) = rw(\mathbf{n})$. This can be written as

$$w(\mathbf{x}) = v^*(\mathbf{x}) = \sup_{\mathbf{p}} \{\mathbf{p} \cdot \mathbf{x} - v(\mathbf{p})\}.$$

The mapping $v \rightarrow w = v^*$ is called the *Fenchel Transform* (or *Legendre Transform* when v is differentiable); the Fenchel transform of $w = v^*$ takes one back to v . Thus the "Wulff shape" for the function w is the plot of $\mathbf{n}/v(\mathbf{n})$; Frank refers to this plot as the pedal of W_∞ [41].

When v is not a convex function, the plot of ∇v (interpreted as above) coincides with the surface of its W_∞ except for additional "ears" at corners and/or edges of W_∞ (as is the case for a surface energy function γ and its Wulff shape W).

3.1.1. The question of regularity: shocks and fans.

We see that there are several ways in which the construction of solutions via characteristics can fail to cover cases we would like to consider. The first is that we want crystal growth to be determined for all positive time (including when characteristics cross). The second is that we want to consider growth velocities v that may be continuous with respect to normal direction but not have a continuous gradient. (As we will see, such discontinuities in the gradient of v do occur at facet orientations of W_∞ .) The third is that we want to be able to use initial shapes with corners and edges. These issues are resolved by the use of shocks and fans, provided we assume that both our initial surface and v are continuous everywhere and piecewise C^2 (i.e. first and second derivatives are piecewise continuous). We describe their use below; also see Haberman's undergraduate-level textbook exposition of shocks and fans [102].

A shock occurs when two or more characteristics arrive at the same point at the same time. Thus the need for introducing shocks can be detected by plotting all characteristics as if they extended for all time, and seeing where characteristics cross. All characteristics encountering a shock are terminated, and give no information about future growth. A shock results in a discontinuity, in this case in ∇v and in \mathbf{n} as well, and thus gives rise to a corner or an edge on the crystal surface. The jump condition at a shock is determined from the physics of the problem, not the PDE; here the physics requires that the crystal surface [as determined by the points $\mathbf{x}(t)$ the characteristics reach at time t] be continuous, and (provided v is positive) that once the crystal has grown past a point, that point should remain part of the crystal. (Sethian [4, 5] formulated this condition for flame propagation as "once burned, stays burned.") Differentially, our shock condition at a point \mathbf{x} along a shock between normals \mathbf{n}_α and \mathbf{n}_β is, in two dimensions, that

$$d\mathbf{x}/dt = s_\alpha \mathbf{t}_\alpha + \nabla v(\mathbf{p}_\alpha) = s_\beta \mathbf{t}_\beta + \nabla v(\mathbf{p}_\beta)$$

where \mathbf{t}_α is a unit tangent vector to the α surface and is thus perpendicular to \mathbf{p}_α , \mathbf{t}_β is defined similarly for the β surface, and s_α and s_β are numbers determined by solving the vector equation (which is a system of two linear equations in those two variables). [In the

special case where each gradient vector lies in the other surface's tangent half plane, this becomes

$$dx/dt = \nabla v(\mathbf{p}_\beta) + \nabla v(\mathbf{p}_\alpha).]$$

In three dimensions, at a point in an edge of a growing crystal we have three naturally defined tangent vectors, one along that edge and the other two perpendicular to it and into the two surfaces meeting along that edge. The equation for dx/dt is similar to the above, except there are two s 's for the α side and two for the β side. The three dimensional vector equation thus yields three linear equations in four unknowns, but the extra degree of freedom corresponds to the fact that one has a *shock surface* rather than a shock line emanating from an edge, and the degree of freedom is in the direction of the tangent line to the edge. At a corner where three surfaces meet, there are six s 's and two three-dimensional vector equations, yielding six equations in six unknowns, and thus a differential equation for the propagation of the corner. If a corner with more than three surfaces is to propagate, then special relations must exist among the $v(\mathbf{n})$ s in order to enable a solution to the equations to exist; this can happen in crystals because of their symmetry. (In order for such a shock to form with more than three surfaces related by symmetry, there must be appropriate symmetry in the initial crystal shape as well.) Note that shocks in particular appear when a nonconvex crystal grows so that two different portions of surfaces come into contact and merge, changing the topology of the surface. At that instant, the shock starts from the contact point and spreads out all around it. If contact occurs on a whole piece of surface at a given time (so that that piece of surface is instantly annihilated), then all the characteristics going into that piece of surface from both sides terminate. (Mathematically, the crystal surface itself is assigned to the crystal—the region which grows when $v > 0$ —rather than the complementary region, in order that if contact occurs on a whole piece of surface, that portion automatically disappears into the interior of the crystal.) Similarly, all remaining characteristics collide and terminate at the instant that a hole in a crystal (or a dissolving crystal) disappears.

If there is a point on the crystal with normal \mathbf{n}_0 and v has a discontinuous gradient at \mathbf{n}_0 , then in place of ∇v one uses all the convex combinations of the limits of $\nabla v(\mathbf{n})$ as the normals \mathbf{n} approach \mathbf{n}_0 —i.e. all the vectors in the *subgradient* of v at \mathbf{n}_0 . Thus a whole “fan” of characteristics leaves such a point. An example in which this happens is where $v_{\text{cube}}(\mathbf{n}) = |n_1| + |n_2| + |n_3|$ and where the initial surface is a sphere. The fans result in facets developing along the coordinate axes. In situations where a facet already exists with direction \mathbf{n}_0 where ∇v is discontinuous, then there are fans of characteristics emitted from each point in the facet, and fans from neighboring points in the facet cross each other. It is as if there is a whole continuum of shocks. (In fact, it is even

worse than that—each individual characteristic need not be determined by the initial choice of element of the subgradient but can make any choice at any later point along the characteristic, so that the set of all characteristics from a point includes the set of all *Lipschitz paths* with their tangent rays at each point being some element of the appropriate subgradient.) However, they all in fact give the same two items of information: the facet is moving forward at velocity $v(\mathbf{n}_0)$, and is spreading out no further than the rate allowed by the outer characteristics of the fans. It may well spread out much less than that due to shocks at the edges of the facet—in fact, the entire fan might be cut off by a shock, and will be, if v is a *convex function* and if the surface near the point with normal \mathbf{n}_0 is not convex.

Another place that fans of characteristics are used is at points on the initial surface where there are corners or edges such that the limiting normal directions as the corner or edge is approached do not all have the same value of ∇v . Here there are often several ways that the surface can evolve while still satisfying the PDE at the regular points. For example, suppose that v is isotropic with value 1 in all directions, and suppose that the initial shape is a cube. An evolution that apparently satisfies the equation of motion is for the cube to simply expand in size with time, resulting in the edges moving at a net velocity of $\sqrt{2}$ and the corners at a net velocity of $\sqrt{3}$. However, if the corners were slightly rounded initially, the rounded portions would grow with velocity 1, not $\sqrt{3}$, and this appears to be the most physically realistic solution, since it is stable under perturbations. It is also the solution that one gets by putting in a fan of characteristics at each edge and corner, using all the values of $\mathbf{n}[\equiv \nabla v(\mathbf{n})]$ which are omitted at that edge or corner. This, however, is an issue that needs to be settled by experiment.

If v is a convex function, then at nonconvex corners and edges these fans will be immediately cut off by shocks (and so need not have been introduced at all), while they will definitely be required at convex corners and edges in order to determine the growth via characteristics. But when v is not a *convex* function, which is quite possible physically, the situation is more complicated, and the use of characteristics can fail to give a unique solution. For example, as described in Section 4 below, if $v(\mathbf{n}) = (1 + \alpha)(|n_1| + |n_2| + |n_3|) - \alpha \max\{|n_1|, |n_2|, |n_3|\}$ for some $\alpha > 0$, then a concave corner formed by planes with normals $(1, 0, 0)$, $(0, 1, 0)$ and $(0, 0, 1)$ would satisfy the evolution equation on its regular parts if the three plane segments just translated, each with velocity 1, via use of the fans of characteristics from each point in each segment; shocks would form at the pairwise intersections of the segments. There are several other solutions, however. In particular, if fans of characteristics are introduced for the omitted values of ∇v at the edges and corners, then one could

form a different set of shocks involving these directions as well, and get an evolution which put in facets with normals $(1, 1, 0)$, $(1, 0, 1)$ and $(0, 1, 1)$, growing with normal velocity $\sqrt{2 + \alpha}$, along the edges and an additional facet with normal $(1, 1, 1)$ growing with normal velocity $\sqrt{3 + 2\alpha}$ from the corner. Again, the appropriate condition to use when solutions are non-unique seems to be that a solution be stable under perturbations (in the sense that a perturbation to such a solution will not grow without bound). In the above case, this condition would produce the latter evolution. This, however, is again an issue that needs to be settled by experiment.

Here is a procedure to determine the growth from at least some corners \mathbf{x}_0 of the initial surface C_0 , using characteristics, in such a way that the stability condition is satisfied. Look at the *tangent cone* (the set of all the rays from \mathbf{x}_0 tangent to C_0) at a point \mathbf{x}_0 which is on an edge or in a corner of C_0 . This tangent cone is composed of pieces of planes. (Any curved portion of the tangent cone would entail infinite curvature at \mathbf{x}_0 , violating our piecewise C^2 hypothesis.) For each \mathbf{y} in the tangent cone such that there is a normal \mathbf{n}_y to the tangent cone at \mathbf{y} , plot $\mathbf{y} + t\nabla v(\mathbf{n}_y)$ for $t = 1$. At each point \mathbf{y} in an edge or corner of the tangent surface, plot $\mathbf{y} + t\nabla v(\mathbf{n})$ for $t = 1$ and all \mathbf{n} omitted at that edge or corner. Note the similarity to Huygens' wavefront construction [100]. The resulting surface will be continuous, because we use the subgradient where ∇v is discontinuous, but it may be self-intersecting. Now at convex portions of the tangent cone, discard all the fan characteristics whose directions come from concave portions of the plot of ∇v , and at concave portions of the tangent cone, discard all the fan characteristics whose directions come from convex portions of the plot of ∇v . From the remaining characteristics, the inner envelope is taken for convex corners and the outer envelope for concave corners. At saddle-shaped corners things are more complicated. If only three plane segments meet at such a corner, and if the evolution produces no new orientations along the edges, then no new orientations need be introduced at the corner itself—the characteristics to be used are those which result in a translation of the corner. Somewhat more generally, for any saddle-shaped corner there are directions in which the surface bends in a convex manner and directions in which it bends in a concave manner. One need keep characteristics for omitted directions at that corner only if v is convex in the directions in which the surface is convex and is concave in the directions in which the surface is concave. A major advantage of the formulation of the problem in terms of viscosity solutions rather than characteristics is that one is guaranteed the existence of a unique solution; furthermore, this solution satisfies the stability condition. Also, the computational methods based on this viscosity-solution formulation

automatically find it. One need not specify the details of the shocks and fans when working with viscosity solutions.

In our previous paper [2], many examples were given of the use of characteristics, including their use in a fixed temperature gradient and with velocity functions that change sign (and hence are zero in places). Also, several physical situations were discussed where the method of characteristics can be used, including discontinuous coarsening and diffusion-induced recrystallization. But beware—in our previous paper [2] we guessed that the stability shock condition might be equivalent to the condition that the crystal grow as fast as possible, subject to continuity. This is incorrect; it is possible that at a sharp convex corner which cuts off two corners and an intervening smooth region of the plot of ∇v , a fast growth shape could form using a shock between characteristics from the outer parts of the two corners, whereas the stable growth pattern would be the slower one using two shocks and the fan of characteristics corresponding to the smooth omitted region.

3.2. Level sets of viscosity solutions of certain PDEs

We discuss here the method of viscosity solutions of PDEs of the form

$$u_t - |\nabla u| M(-\nabla u / |\nabla u|) \times \left\{ \Omega - \sum_{i=1}^3 \frac{\partial}{\partial x_i} \left[\frac{\partial}{\partial p_i} \gamma(\mathbf{p})_{\mathbf{p} = -\nabla u / |\nabla u|} \right] \right\} = 0$$

$$u(\mathbf{x}, 0) = a(\mathbf{x})$$

where γ is C^2 and strictly convex [and extended by $\gamma(\mathbf{p}) = |\mathbf{p}| \gamma(\mathbf{p}/|\mathbf{p}|)$ to non-unit vectors]. This is the form that our basic velocity equation takes when it is put in the general indirect formulation for the normal velocity. All of the minus signs are there because we are following the convention as in Section 1 that u be positive on the “inside” region and also taking the normal of that region to be the exterior normal, so that $\mathbf{n} = -\nabla u / |\nabla u|$.

As stated in Sections 1 and 2, the function u here has no particular physical meaning and its only purpose is to define the crystal surface at time t as the level set $u(\mathbf{x}, t) = 0$. The function a which specifies the initial values is chosen so that the zero level set of a is the crystal surface at time $t = 0$.

Note that if the PDE is satisfied by u , it is also satisfied by $w = f(u)$ for any differentiable function f , since $\partial w / \partial t = f'(u) \partial u / \partial t$ and $\nabla w = f'(u) \nabla u$. Furthermore, u and $f(u)$ describe the same crystal growth if f is strictly increasing (or decreasing), in the sense that for any constant c ,

$$\{\mathbf{x} : u(\mathbf{x}, t) = c\} = \{\mathbf{x} : f(u(\mathbf{x}, t)) = f(c)\}.$$

If one only wishes to track one level set, e.g. $u = 0$, then one can specify $u(\mathbf{x}, 0) = a(\mathbf{x})$ for any continuous function $a(\mathbf{x})$ such that the set of points \mathbf{x} where $a(\mathbf{x}) = 0$ is the desired initial surface. There are

infinitely many choices of function $a(\mathbf{x})$ which satisfy $a(\mathbf{x}) = 0$ precisely on the crystal surface at time $t = 0$. Nevertheless, it is a theorem that *all* choices of continuous a with $a(\mathbf{x}) = 0$ on just the given initial surface will produce the same sets $\{\mathbf{x}: u(\mathbf{x}, t) = 0\}$ at all subsequent times t (assuming that $\Omega = 0$; for non-zero Ω , one must also specify where $a > 0$ and where $a < 0$). It is not clear whether one can choose $a(\mathbf{x})$ to have any physical meaning off the zero set at time $t = 0$ apart from determining the set where it is zero, in such a way that $u(\mathbf{x}, t)$ continues to have that meaning at later times; however, in terms just of computing the crystal growth, there would not be any advantage in making such a choice even if there were one. [One might like to have $a(\mathbf{x})$ be the time at which the crystal surface first passes \mathbf{x} , but among other problems that would require knowing the solution for all time at time $t = 0$, instead of using the PDE to find the solution.]

There are advantages to writing the equation in this form, in addition to that of obtaining a single equation which is valid for positive, negative or zero velocity. A significant one from the point of view of writing proofs is that one doesn't have to worry separately about the problems caused by non-smoothness, either of the mobility function M or of the initial surface or of the surfaces which develop at later times. The definition of the viscosity solution enables one to prove existence and uniqueness of solutions for all times. It also turns out (as we will show below) that for the motion of a single interface by a prescribed velocity as a function of normal direction alone, the concept of the "viscosity solution" to the PDE above is precisely the one we want. For example, the method of characteristics, applicable only when $\gamma \equiv 0$, can give multiple solutions for corners and edges. That definition of the viscosity solution enables one to find which particular evolution of a given corner is the correct one. This is demonstrated below in Section 4 for several examples.

Furthermore, in this case of $\gamma \equiv 0$, the viscosity-solution definition enables one to check fairly easily whether a particular evolution of a given corner is the correct one, when multiple solutions are given by the method of characteristics, as we shall demonstrate later.

Viscosity solutions have certain advantages over the other methods. For example, in case γ is not everywhere zero, the method of characteristics is not applicable (the equation may be quasilinear and parabolic, but it is *degenerate elliptic*), and singularities such as develop when necks pinch off cannot be handled through the classical mapping approach. Since the level-set-of-a-function approach still works and the viscosity solution is also the physically reasonable one except in the presence of certain types of junctions of pieces of surface, this method is particularly powerful. (It may be that if such junctions are not part of the initial data, then they

never occur at later times, although no-one has yet succeeded in proving this.)

Another advantage to the level-set-of-a-function formulation is that it lends itself to numerical calculation. In fact, a way to obtain numerical solutions (whether by tracking the surface or by solving for a global u) to the problem where v is a function of normal direction alone is to add to the PDE a curvature-dependent term times ε [6]. Solutions to the modified problem do not develop shocks except as a result of topological changes. There is a large overhead to writing the PDE in terms of u for such computations, as one must compute $u(\mathbf{x}, t)$ for all \mathbf{x}, t even though one cares only about the set of points \mathbf{x} at time t where $u(\mathbf{x}, t) = 0$. Still, it can be much simpler than trying to determine where shocks occur and how to track them, especially when the topology of the crystal changes (e.g. necks break off or form, holes close off or form, etc.).

There are some corresponding disadvantages to thinking about the problem of solving

$$\partial u / \partial t - v(\mathbf{x}, t, -\nabla u) = 0$$

rather than

$$1 - |v(\mathbf{x}, \tau, \pm \nabla \tau)| = 0.$$

One is that the solution becomes something much more abstract than easily-visualized characteristics. In fact, there are no general results that say that the result is a surface at each time. In particular, it is known that sometimes the surface (the set where $u = 0$) can smear out over a whole region [7] (see the example at the end of Section 4). (There is another formulation [11], where one looks just at boundaries of sets; this formulation avoids the spread-out regions but loses uniqueness.) Another disadvantage, as mentioned above, is that one must compute information that is really unnecessary, i.e. the values of u where u is non-zero. The most fundamental problem occurs, however, when one wants to consider three or more regions, so that there are three or more types of surfaces, each moving with some velocity, and at least one triple junction where all three phases meet. One would have to go to a PDE with vector values to produce a physically realistic solution in this case.

We now proceed to define viscosity solutions of certain PDE, following [1]. The type of PDE we consider is

$$\partial u / \partial t + F(t, \mathbf{x}, \nabla u, \nabla^2 u) = 0$$

where $\nabla^2 u$ means the Hessian matrix of second partial derivatives of u in the spatial variables, and F is required to be *geometric* and *degenerate elliptic*. It has been shown that F being degenerate elliptic and geometric (more specifically, strongly geometric [105]) implies that the normal velocity v of the level sets of u comes from geometric interface evolution, so that it is a function of $t, \mathbf{x}, \mathbf{n}$ and the gradient of \mathbf{n} [105].

Our case of interest can be written in this way if γ is C^2 and strictly convex, with

$$F(t, \mathbf{x}, \mathbf{p}, X) = |\mathbf{p}|M(\mathbf{x}, t, -\mathbf{p}/|\mathbf{p}|) \times \{\Omega(\mathbf{x}, t) + \text{trace}[A(\mathbf{p}/|\mathbf{p}|)X/|\mathbf{p}|]\}.$$

Here $A(\mathbf{p})$ is the matrix of second derivatives of γ . Note that when γ is isotropic, A is the identity matrix and the term involving A is the divergence of the normal vector, which is the mean curvature. For anisotropic γ , that term is the weighted mean curvature. (See the following paper.)

For a degenerate elliptic PDE with a geometric F , a continuous function u is defined to be a *viscosity subsolution* of

$$\partial u/\partial t + F(t, \mathbf{x}, \nabla u, \nabla^2 u) = 0$$

if for each (\mathbf{x}_0, t_0) with $t_0 > 0$ and each twice-differentiable test function $\phi(\mathbf{x}, t)$ satisfying

$$u(\mathbf{x}, t) - \phi(\mathbf{x}, t) \leq u(\mathbf{x}_0, t_0) - \phi(\mathbf{x}_0, t_0)$$

for all \mathbf{x}, t , it holds that

$$\frac{\partial \phi}{\partial t}(\mathbf{x}_0, t_0) + F[\mathbf{x}_0, t_0, \nabla \phi(\mathbf{x}_0, t_0), \nabla^2 \phi(\mathbf{x}_0, t_0)] \leq 0$$

and u is a *viscosity supersolution* if whenever

$$u(\mathbf{x}, t) - \phi(\mathbf{x}, t) \geq u(\mathbf{x}_0, t_0) - \phi(\mathbf{x}_0, t_0)$$

for all \mathbf{x}, t , then

$$\frac{\partial \phi}{\partial t}(\mathbf{x}_0, t_0) + F[\mathbf{x}_0, t_0, \nabla \phi(\mathbf{x}_0, t_0), \nabla^2 \phi(\mathbf{x}_0, t_0)] \geq 0$$

u is defined to be a *viscosity solution* if it is both a viscosity subsolution and a viscosity supersolution of that PDE. (To handle possible problems at $\mathbf{p} = 0$, a slightly more elaborate definition actually needs to be used [1].)

To understand intuitively what viscosity solutions are, first note that if the solution u is twice differentiable, it can itself be used as a test function ϕ , for both the subsolution test and the supersolution test, and thus u itself must satisfy the PDE. Thus the only purpose of viscosity solutions is to make sense of what it means for u to satisfy the PDE when u cannot be differentiated and plugged into the equation. In particular when there are corners and edges in the level set $u = 0$, one cannot check that u is a solution by putting it in the PDE.

Built into the definition is the idea of “barriers,” in that smooth solutions which are initially completely “behind” [resp., “in front of”] the surface, and which remain behind [resp., in front of] at one point for later times, in fact remain behind [resp., in front of] everywhere for later times. They thus embody the idea of being stable to perturbations. An odd fact is that if we were to replace the PDE by its negative, then the PDE remains the same, but the viscosity solutions would change. The reason is that the viscosity solution picks out one solution among many possibilities when there is non-smoothness, and

since it picks one that “goes farthest” when the equation is written one way, it will not necessarily go farthest when it is written in another way. Thus the way the equation is written when the problem is formulated is crucial to get the physically desired solution.

An apparent disadvantage of using viscosity solutions is that the definition itself seems quite roundabout and awkward, but in practice it is often relatively easy to use for disproofs and even proofs, provided one can find a way to deal with “every test function.” While a single counterexample to either the sub- or supersolution test is sufficient to prove that u is not a solution, often the non-existence of a suitable test function is a complete and easy test. Note that there are NO continuously differentiable functions which agree with u on a corner or edge of the cube and which are bounded above by u in a neighborhood of such a corner. Thus at the corner, u automatically passes the supersolution test. In fact, any corner or edge in a level set will automatically pass either the subsolution or the supersolution test (or both, for a saddle-shaped corner); this is one of the major advantages of the viscosity solution approach [1].

In most cases of interest here, it is sufficient, according to a theorem of [10], to do the tests with just linear comparison functions. Specifically, u is a viscosity solution of a first-order PDE $G[\mathbf{y}, u(\mathbf{y}), Du(\mathbf{y})] = 0$ [for us, $\mathbf{y} = (\mathbf{x}, t)$, $Du(\mathbf{y}) = (\nabla u, u_t)$, and $G = u_t - v(\mathbf{x}, t, \nabla u)$] if and only if

$$G[\mathbf{y}, u(\mathbf{y}), \mathbf{p}] \leq 0 \quad \forall \mathbf{y}, \forall \mathbf{p} \in D^+ u(\mathbf{y})$$

and

$$G[\mathbf{y}, u(\mathbf{y}), \mathbf{p}] \geq 0 \quad \forall \mathbf{y}, \forall \mathbf{p} \in D^- u(\mathbf{y})$$

where $D^+ u(\mathbf{y}_0)$ is the set of all \mathbf{p} such that

$$\limsup_{\mathbf{y} \rightarrow \mathbf{y}_0} [u(\mathbf{y}) - u(\mathbf{y}_0) - \mathbf{p} \cdot (\mathbf{y} - \mathbf{y}_0)] |\mathbf{y} - \mathbf{y}_0|^{-1} \leq 0$$

and $D^- u(\mathbf{y}_0)$ is the set of all \mathbf{p} such that

$$\liminf_{\mathbf{y} \rightarrow \mathbf{y}_0} [u(\mathbf{y}) - u(\mathbf{y}_0) - \mathbf{p} \cdot (\mathbf{y} - \mathbf{y}_0)] |\mathbf{y} - \mathbf{y}_0|^{-1} \geq 0.$$

Here \limsup means the largest possible limit to any subsequence and \liminf means the smallest possible limit; even if a sequence doesn't converge, it always has a \limsup and a \liminf (which may be infinite).

What that says is that for a first order PDE only the first-order behavior matters. When the velocity does not depend on the derivative of the normal vectors, we need really look only at once-differentiable comparison functions. Where linear functions satisfy the appropriate inequality, it is sufficient to use them; higher order terms will contribute nothing meaningful to the tests. Thus we really have to concern ourselves only with corners and edges, and only in the directions for which a linear comparison function can be constructed. (There is also a similar reformulation in terms of “jets” for second order PDEs.)

Examples of the use of viscosity solutions are in Section 4.

3.3. Crystalline method

The *crystalline method* converts the PDE problem of the mapping method [method (1)] into the system of ordinary differential equations (ODEs) stated below. These equations can easily be solved numerically (and sometimes analytically). The method can handle fixed boundaries and multiple grains or phases and changes of topology [17].

It applies if one assumes that the surface energy γ and the mobility M are each given only on a certain common finite set of normal directions $\{\mathbf{n}_\alpha\}$, and that when the Wulff construction is performed using these values of γ to get W , each plane $\mathbf{x} \cdot \mathbf{n}_\alpha = \gamma(\mathbf{n}_\alpha)$ intersects W in a complete facet, a complete edge, or just a corner. Similar restrictions need not be made on the values of $M(\mathbf{n}_\alpha)$.

Alternatively, one can have γ and M be defined on all vectors, provided there exists a set $\{\mathbf{n}_\alpha\}$ such that the value of γ on these vectors satisfies the above conditions and the W computed from the values of γ on these vectors is the same as that computed using the values of γ on all vectors, and provided that for each unit vector \mathbf{n} not in $\{\mathbf{n}_\alpha\}$, $M(\mathbf{n})$ is precisely the value determined by linear interpolation between the values of M on the pair (in 3-d, usually triple) of vectors in $\{\mathbf{n}_\alpha\}$ nearest \mathbf{n} with \mathbf{n} in their span. We require this compatibility condition in order that a segment with a normal not in the $\{\mathbf{n}_\alpha\}$ set moves with the same mobility whether or not it is considered as an infinitesimally corrugated varifold.

The crystalline method is therefore applicable for a material such that the Wulff shape is a polyhedron. Although the word “crystalline” is used here, there are of course many crystalline substances whose Wulff shapes are not polyhedra. Also, the crystalline method should be a useful tool for approximation for arbitrary γ .

The set of vectors $\{\mathbf{n}_\alpha\}$ form the vertices of an n -diagram [120, 121] on the unit sphere. When two vertices are normals of adjacent facets, there is a tie-line (great circle segment) between vertices in the n -diagram and these tie-lines divide the sphere up into regions. Any \mathbf{n}_α in the specified set whose plane intersects W only in an edge is in the tie-line corresponding to that edge, and any that intersects W only in a corner is in the tie region corresponding to that corner.

The type of initial data that is easiest to handle is a polygonal surface where the normal of each facet is in the set $\{\mathbf{n}_\alpha\}$, and where adjacent facets correspond to vertices on a single tie line in the n -diagram with no intervening vertices, and (in 3-d) three plane segments meet at each corner, and if that corner is convex or concave rather than saddle-shaped, then there are no vertices inside the triangle of the n -diagram formed by those three vertices. Such a surface will be called a *good* surface.

We consider first the case that $\gamma \equiv 0$. Then the motion of a *good* surface is determined by translating the segments of the surface the appropriate distances along their normals, extending or truncating them so that they maintain the same combinatorial structure. That is, if s_i is the distance of the plane containing segment S_i from the origin and \mathbf{n}_i is its normal, the growth law is just

$$ds_i/dt = \Omega M(\mathbf{n}_i)$$

for each i ; this trivially integrates to

$$s_i(t) = s_i(0) + t\Omega M(\mathbf{n}_i).$$

Coordinates of corners are determined by solving the appropriate set of simultaneous linear equations. The only time the structure can change is when segments, or portions of segments, are squeezed out by the growth of their neighbors or when different portions of surface collide; this makes shocks form, in the language of characteristics. Checking for such events is relatively simple, given the finiteness of everything, so the computational disadvantages of having to find and track shocks are greatly ameliorated in this case. Motion with $\gamma \equiv 0$ is thus the same as would be predicted by the use of characteristics with this velocity ΩM , but it can be computed in a much simpler fashion. In case $\gamma \neq 0$, weighted mean curvature can be defined for polyhedral surfaces, not by differentiating but by going back to the idea that, for 2-dimensional surfaces, the mean curvature is the rate of decrease of surface energy with respect to volume under deformations (small pushes) of the surface. (For 1-dimensional curves in the plane, it is the rate of decrease of line energy with respect to area under deformation [34].) For a *good* surface, one computes, as in Gibbs, that the weighted mean curvature of segment S_i (having normal \mathbf{n}_i) should be defined to be

$$-\frac{1}{\text{area}(S_i)} \sum_{j \neq i} \delta_{ij} f_{ij} l_{ij}$$

where l_{ij} is the length of the intersection of segment S_i and S_j (and is thus 0 if those segments are not adjacent in the interface), δ_{ij} is 1 or -1 , depending on whether the type of the $S_i - S_j$ edge is *regular* (like that in W) or *inverse* (like that in the central inversion of W), and f_{ij} is a numerical factor determined by the geometry of W , namely

$$f_{ij} = [\gamma(\mathbf{n}_j) - c_{ij}\gamma(\mathbf{n}_i)] / \sqrt{1 - c_{ij}^2}$$

where $c_{ij} = \mathbf{n}_i \cdot \mathbf{n}_j$. In 2-d, $\text{Area}(S_i)$ is replaced by length (S_i) , l_{ij} disappears, and the sum $\sum_j \delta_{ij} f_{ij}$ has only two terms and can be simplified to $\sigma_i \Lambda(\mathbf{n}_i)$, where $\Lambda(\mathbf{n}_i)$ is the length of the segment in the Wulff shape W with normal \mathbf{n}_i , and σ_i is 1 if both ends of the segment are of regular type, -1 if both ends are inverse type, and 0 if the ends have different types.

Thus in 2-d and with the assumption that the initial surface is *good*, motion by weighted mean curvature

(with the velocity additionally weighted by mobility) simply consists of moving line segments according to

$$ds_i/dt = -M(\mathbf{n}_i) \frac{\sigma_i \Lambda(\mathbf{n}_i)}{\text{length}(S_i)}$$

and the general law for geometric growth becomes

$$ds_i/dt = M(\mathbf{n}_i) \left[\Omega - \frac{\sigma_i \Lambda(\mathbf{n}_i)}{\text{length}(S_i)} \right].$$

The same combinatorial structure is maintained until a segment is reduced to zero length or collides with another segment. For motion by weighted mean curvature alone ($\Omega = 0$), such reduction to zero length occur only in the merging of the two adjoining line segments to one or in the total disappearance of a curve due to all edges becoming of zero length at once. But collisions can occur, if $\Omega \neq 0$, or if $M(\mathbf{n}) \neq M(-\mathbf{n})$, or if the Wulff shape does not have a center of symmetry. The resulting cancellation and separation into two curves usually leads to *bad* corners (i.e. ones whose normal directions are not adjacent in the Wulff shape, and which are thus not locally minimizing). Also, if $\gamma \equiv 0$, line segments can shrink to zero length without the whole curve disappearing. (And, as a mathematical aside, the initial curve might cross over itself—which is of course impossible for a crystal surface or grain boundary—and then individual loops of a curve can shrink to zero size without the rest of the curve disappearing.) Since bad corners usually form at all such times, it is important to know how to evolve them. Fortunately, it turns out that if the missing orientations are inserted with “infinitesimal” length at such bad corners, then there is a unique evolution of these segments, and it can be found computationally to any desired degree of accuracy.

In 3-d with $\gamma \neq 0$, one needs somewhat more than just that all edges and corners are good, because plane segments which are “monkey saddles” (with three up-and-down waves around them, rather than the two of a standard saddle) or which have two adjacent convex corners can split and because extra facets may need to be introduced along edges with adjacent convex corners. The precise determination of when such splittings and introduction of new facets is necessary is still being investigated. However, once all necessary facets have been introduced, the motion is again just by moving plane segments while keeping the same combinatorial structure, according to the law

$$ds_i/dt = M(\mathbf{n}_i) \left[\Omega - \sum_{j \neq i} \delta_{ij} f_{ij} l_{ij} / \text{area}(S_i) \right].$$

Again, one has to detect and treat the cases of collisions and facets shrinking to zero width.

Since one can always approximate a smooth W by a polyhedron and a smooth surface by a polygonal one, this crystalline method should be usable for all surfaces and surface energy functions, but the

nature of that approximation is just beginning to be investigated.

To extend the definition of motion by crystalline curvature to the case where there are junctions of three or more curves, one recasts the problem as a variational problem as described in the following paper [34]. First, for a polygonal curve, if we let h_i be the rate at which facet S_i is to move (so that $ds_i/dt = h_i$) and let l_i be the length of facet S_i , then the variational problem, to first order in Δt , is to maximize

$$\Delta t \sum_i (\Omega l_i h_i - \sigma_i \Lambda(\mathbf{n}_i) h_i),$$

the decrease in total free energy due to moving at that velocity for time Δt , subject to

$$\sum_i [h_i \Delta t / M(\mathbf{n}_i)] h_i l_i = \text{constant}$$

which says that the integral of the driving force over the region swept out by the motion is a prescribed constant. (If no motion can decrease the total free energy to first order, then this is a stationary point of the flow, and one simply sets $h_i = 0$ for all i .) Using a Lagrange multiplier λ , one obtains that for each i

$$\Omega l_i - \sigma_i \Lambda(\mathbf{n}_i) = \lambda 2 h_i l_i / M(\mathbf{n}_i).$$

If one chooses the constant so that $\lambda = \frac{1}{2}$ and solves for the h_i s, one obtains

$$h_i = M(\mathbf{n}_i) \left(\Omega - \frac{\sigma_i \Lambda(\mathbf{n}_i)}{l_i} \right)$$

as desired. Note that the constant is constant only for the variational formulation at a particular time; it can and does change with time to maintain $\lambda = \frac{1}{2}$. In fact, since it is the Lagrange multiplier and not the constant which is naturally prescribed, one is really maximizing the combined quantity

$$\Delta t \sum_i [\Omega l_i h_i - \sigma_i \Lambda(\mathbf{n}_i) h_i] - (1/2) \sum_i [h_i \Delta t / M(\mathbf{n}_i)] h_i l_i.$$

Such an explicit formula for steepest descent in terms of l_i, σ_i , etc. uniquely determines the motion.

For triple junctions, one adds the condition that the three segments continue to meet (e.g. if segments 1,2,3 form a triple junction, then there exists a point \mathbf{p} such that $\mathbf{n}_i \cdot \mathbf{p} = h_i$ for $i = 1,2,3$); the formula for computing the net change in surface free energy also now depends on the new intersection point \mathbf{p} . Because it may be advantageous to add a new infinitesimal line segment at a triple junction, one has to do the maximization over all possible such additions of line segments; the best addition may well be a segment which is a varifold, having a normal which is not in the set $\{\mathbf{n}_\alpha\}$. Luckily for computational purposes, the correct varifold solution can be closely approximated by using small segments of alternating orientations which are in $\{\mathbf{n}_\alpha\}$. This variational approach should give the same result when $\gamma = 0$ as the use of characteristics or the least

time formulation [15], and unpublished work of Taylor shows that this is true.

4. EXAMPLES OF USE OF THE VARIOUS METHODS

In this section we examine how a variety of simple problems would be solved by more than one method. By comparing the list of conditions under which various methods apply (2.1.1), one can see that no problem can be solved by all methods. In particular, the direct mapping theory cannot be used for polyhedral initial surfaces. These simple problems are contrived in that the solutions can be found "by hand." They serve to illustrate the various methods, and show that the methods differ enormously in ease of use but on typical problems give identical results. The only case in which different results are known to arise when two different methods apply is exemplified by motion by mean curvature with a non-embedded initial surface such as a figure 8 curve in 2-d; this case is briefly discussed at the end.

4.1. Isotropic constant normal growth from a cube ($\gamma \equiv 0$)

In the isotropic normal growth case, with no curvature dependence, the normal velocity is $v = M\Omega$, with M independent of \mathbf{n} . We arbitrarily take $M = 1$ and $\Omega = \pm 1$, so that $v = 1$ corresponds to growth in the direction of \mathbf{n} and $v = -1$ corresponds to shrinking (which is growth in the direction of $-\mathbf{n}$). We demonstrate several methods with an initial shape which is a cube, oriented so that the unit normal vectors point outward. Note that the growth of a cube by simply scaling it, so that it expands linearly in time while remaining a cube, appears to satisfy the requirements of being a solution: it has the property that at each point on the surface at each time t , the normal velocity is 1. The problem is that there is no particular physical or mathematical justification for just extending the sides until they meet. This "solution" also does not satisfy the criterion of being stable under perturbation (here, rounding its corners) and it is not the solution that any of our methods will produce.

4.1.1. Characteristics. In this isotropic case, $\nabla M(\mathbf{p})$ evaluated at \mathbf{n} is equal to \mathbf{n} , which is 1 in magnitude and parallel to \mathbf{n} . The limiting outward growth form W_∞ is a unit sphere; any starting finite shape growing outward will eventually tend to a sphere. With $v = 1$, the faces of the initial cube will grow by translation without an area increase, the fans on edges and corners will round the edges into growing cylinders, and the eight corners will grow octants of spheres. After a large enough elapsed time the corner spherical pieces will dominate, so that it will look like a sphere, but in fact at each time t the surface will consist of eight spherical pieces (each of radius t) with different centers (the corners of the original cube), and there

will be cylindrical strips (of radius t) separating the eight octants, with six flat facets of side length $2t$ joining the flat sides of the cylindrical strips.

With $v = -1$, all the characteristics (including the fans) point inward from the surface instead of outward, and they cross to create shocks at the corners and edges. These shocks at time t go through the corners and edges of a cube with vertices $[\pm(1-t), \pm(1-t), \pm(1-t)]$, and thus the crystal at time $0 < t < 1$ is that cube of side length $2(1-t)$.

In general, corners and edges that are convex in the growth direction become rounded through the fans that originate at them, while corners and edges growing in the concave direction remain sharp; the fans are continually cut off by the shocks.

Since characteristics are least-travel-time paths from their initial point, and since the shock condition is to use the characteristic that first reaches a point, the least-time solution is that given by characteristics. Alternatively, one can directly look for least-travel time paths to demonstrate that a given evolution is indeed the correct solution.

4.1.2. Viscosity solution. We next demonstrate that the cube growing from an initial cube is not a viscosity solution of the appropriate Hamilton-Jacobi equation, whereas the shrinking cube is a viscosity solution.

The PDE for u is written as $u_t - v|\nabla u| = 0$ (and must not be written as $-u_t + v|\nabla u| = 0$; this is one of the peculiarities of viscosity solutions, as noted in section 2.5). We will set up u so that u is positive inside the crystal, which we will take to be the inside of the cube. A cube, with edges parallel to the coordinate axes and with initial size 1, growing or shrinking with unit velocity on each face is the zero set of the function

$$u(\mathbf{x}, t) = vt + 1 - \max\{|x_1|, |x_2|, |x_3|\}$$

where $v = 1$ for the growing cube and $v = -1$ for the shrinking cube for $t \leq 1$; we will restrict ourselves to such u .

We first test whether u is a viscosity supersolution. As noted before, there are no continuously differentiable functions which agree with u on a corner or edge of the cube and which are bounded above by u in a neighborhood of such a corner. Thus at the corners and edges of the cube, u automatically passes the supersolution test.

Let us do supersolution tests for points (\mathbf{x}_0, t_0) [with $\mathbf{x}_0 = (x_{10}, x_{20}, x_{30})$] such that \mathbf{x}_0 is on a face, but not on a corner or edge, of the growing or shrinking cube at time t_0 ; for these \mathbf{x}_0 , $u(\mathbf{x}_0, t_0) = 0$, since the cube surface is the zero set of u at time t_0 . Without loss of generality we choose points on the first quadrant of the (100) face that are not at a corner or edge; in particular, we assume $x_{10} > x_{20} \geq x_{30} \geq 0$. Therefore $x_{10} = 1 + vt_0$ (where $v = 1$ in the growing case and $v = -1$ in the shrinking case). We use comparison functions from inside whose zero level

sets are concentric spheres, tangent to the cube at \mathbf{x}_0 at time t_0 , and growing with normal velocity v , and all centered at $(x_{10} - \varepsilon, x_{20}, x_{30})$, where $\varepsilon = 1 + vt_0 - x_{20}$ is the distance from the nearest edge. This is to ensure that the sphere will stay inside the cube. A ϕ whose level set satisfies these requirements is

$$\phi(\mathbf{x}, t) = \varepsilon + v(t - t_0) - |\mathbf{x} - (x_{10} - \varepsilon, x_{20}, x_{30})|.$$

Then

$$u - \phi = (1 - \varepsilon + vt_0 - \max\{|x_1|, |x_2|, |x_3|\}) + |\mathbf{x} - (x_{10} - \varepsilon, x_{20}, x_{30})| \geq 0$$

[This result, which simply says that the sphere stays inside the cube, is obtained analytically by using the fact that the magnitude of any vector is greater than or equal to that of any of its components; hence, under our assumptions,

$$\begin{aligned} &|\mathbf{x} - (x_{10} - \varepsilon, x_{20}, x_{30})| \\ &\geq \max\{|x_1 - x_{20}|, |x_2 - x_{20}|, |x_3 - x_{30}|\} \\ &\geq \max\{|x_1| - x_{20}, |x_2| - x_{20}, |x_3| - x_{30}\} \\ &\geq \max\{|x_1|, |x_2|, |x_3|\} - x_{20}. \end{aligned}$$

The viscosity supersolution test with ϕ is then whether $\phi_t - |\nabla\phi| \geq 0$ at \mathbf{x}_0, t_0 , and it is. One has to test with *all* ϕ such that

$$(u - \phi)(\mathbf{x}, t) \geq (u - \phi)(\mathbf{x}_0, t_0)$$

for all \mathbf{x}, t , but in fact, as noted in Section 3.2, the above ϕ is sufficiently general for this first-order equation to show that u is a viscosity supersolution.

We now test whether u is a viscosity subsolution. We look first at the corners; by symmetry we need only look at the (1,1,1) corner (the corner in the first octant). For any a, b with $0 < a < 1 - b < 1$, let

$$\phi(\mathbf{x}, t) = 1 + vt - [ax_1 + bx_2 + (1 - a - b)x_3].$$

Then

$$(u - \phi)(\mathbf{x}, t) = -\max\{|x_1|, |x_2|, |x_3|\} + ax_1 + bx_2 + (1 - a - b)x_3 \leq 0$$

with equality when $x_3 = x_2 = x_1 = |x_1|$ —that is, at the first octant corner of the cube, as desired. In the growing case, we have

$$\phi_t - |\nabla\phi| = 1 - |(a, b, 1 - a - b)| > 0$$

which is the wrong inequality; for the shrinking cube, we have

$$\phi_t + |\nabla\phi| = -1 + |(a, b, 1 - a - b)| \leq 0$$

which is the required inequality. Thus the u whose zero level sets correspond to a cube scaling by the factor $1 + vt$ is not a viscosity solution for positive unit normal velocity but is still in contention to be a viscosity solution for negative unit normal velocity.

To complete the verification that u with $v = -1$ is a subsolution, we use similar linear barrier tests

along the edges [$\phi(\mathbf{x}, t) = 1 - t - ax_1 - (1 - a)x_2$] and faces [$\phi(\mathbf{x}, t) = 1 - t - x_1$], obtaining again that $u - \phi \leq 0$ and $\phi_t + |\nabla\phi| \leq 0$.

4.1.3. Crystalline method. The crystalline method does not directly apply to the isotropic case; one can only use it to approximate solutions. Here one might take W_∞ to be a convex polygon approximating a sphere, with $M(\mathbf{n}_i) = 1$ for every normal \mathbf{n}_i to that polygon, and take M to be a convex function.

For $v = 1$, at time 0, facets of all the orientations \mathbf{n}_i that are missing are inserted, at distance $s_i(0) = (1, 1, 1) \cdot \mathbf{n}_i$. Then each of these is moved at normal velocity 1 ($ds_i/dt = 1$). We consider separately the two special cases where (1) the coordinate directions are normals of W_∞ , and there are three families of edges around W_∞ (called zones), the edges in each family being parallel to one of the coordinate axes, and (2) the coordinate axes are perpendicular to neither edges nor facets of W_∞ , and no edge is parallel to the coordinate axes.

In case (1) with $v = 1$, the facets of the cube move outward at normal velocity 1 (expanding somewhat in size), faceted cylinders appear along the edges corresponding to the appropriate quarter circles from the n -diagram, and “octants” of all other directions from W_∞ appear in the corners.

In case (2) with $v = 1$, the facets of the cube translate outward at velocity $a + b + c$ which is slightly greater than 1, where a, b, c , are the coefficients of the expansion of the facet normal in terms of the neighboring normals of W_∞ . “Octants” of W_∞ appear in the corners, with the facets moving at velocity 1. The original facets keep their original size (if M were chosen to be nonconvex, then the original facets would move faster than $a + b + c$ and would eventually be consumed by the facets at the outside of the octants at the corners).

For $v = -1$, facets from W_∞ are again provisionally introduced at the corners and along the edges of the cube, but they do not grow; rather, they are cut off by the motion of the original eight facets. These eight facets grow inward, at unit velocity in case (1) and at velocity $a + b + c$ in case (2), until the cube is completely consumed.

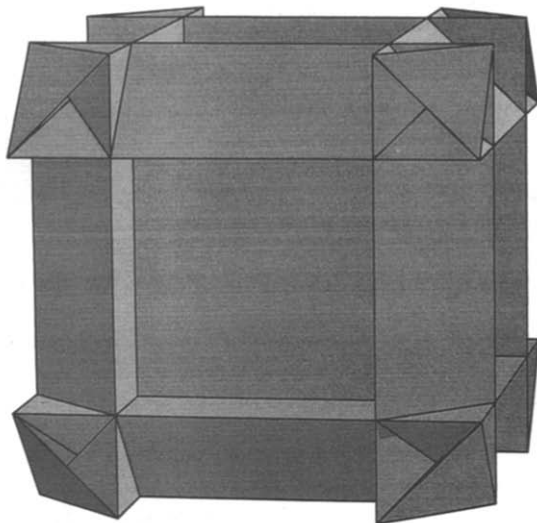
4.2. Anisotropic normal growth from a cube ($\gamma \equiv 0$)

Here we chose any $\alpha > 0$, write $\mathbf{n} = (n_1, n_2, n_3)$, and define the velocity to be

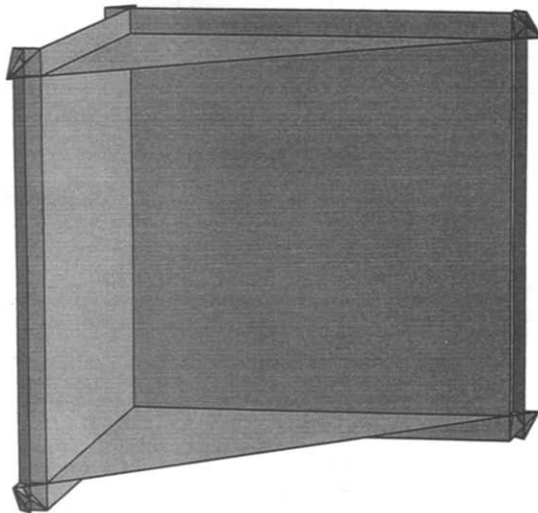
$$M_\alpha(n_1, n_2, n_3) = (1 + \alpha)(|n_1| + |n_2| + |n_3|) - \alpha \max\{|n_1|, |n_2|, |n_3|\}$$

for the growing crystal and to be the negative of this for the shrinking one. Note that $M_\alpha = 1$ on the (100) faces (the faces perpendicular to the coordinate axes), and that M_α is nonconvex (but would be convex if $\alpha = 0$). A plot of all the vectors in all the subgradients of M_α for $\alpha = 0.8$ is in Fig. 1(a).

4.2.1. Characteristics. Note that ∇M_α is constant [it is $(1, \pm(1 + \alpha), \pm(1 + \alpha))$ in each of the four



(a)

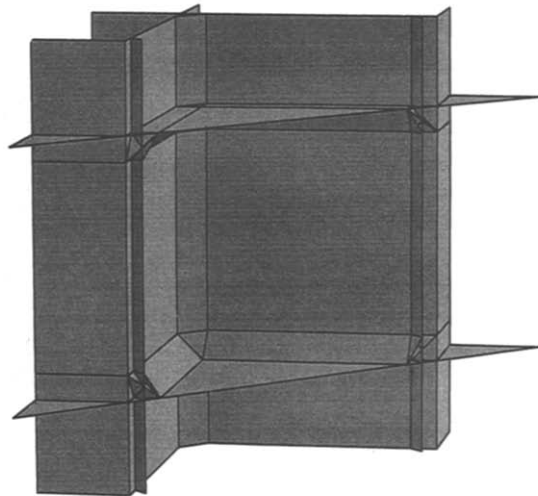


(b)

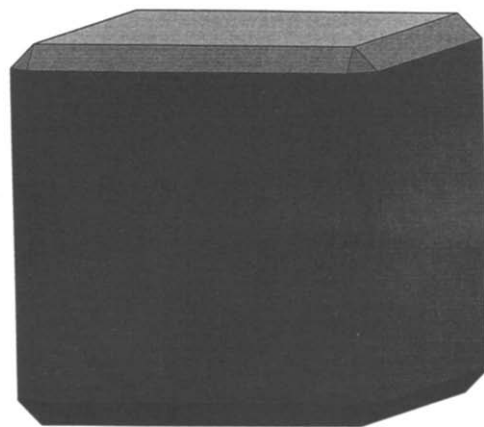
Fig. 1. (a) The plot of all vectors in the subgradient of the M_α of the text is a cube with "ears." (b) With this M_α , the union of the characteristics emanating outward during growth from an initial cube traces out a shape with self-intersections and reentrant corners. A (110) section (through the origin) of the points reached by these characteristics at time $t = 0.2$ (with $\alpha = 0.8$) is shown. Creating the appropriate shocks leaves only a growing cube, whose faces are the cube faces shown, meeting with sharp corners and edges hidden under the to-be-discarded "ears."

open regions of the sphere where $n_1 > |n_2|$ and $n_1 > |n_3|$ but $n_2 \neq 0 \neq n_3$. Thus there are characteristics from all points in the cube face with $x_1 = 1$ which have all directions in the convex hull of those four directions, and at time t the union of all these characteristics goes through all the points in the square with corners $(1 + vt, \pm[1 + t(1 + \alpha)], \pm[1 + t(1 + \alpha)])$. A similar statement holds for the other five facets of the original cube. See Fig. 1(b) for $v = 1$ and Fig. 2(a) for $v = -1$. Note that these

squares intersect each other along line segments where two of the coordinates have absolute value $1 + vt$, but extend past those line segments. From the points on the edge between $(1, 1, 1)$ and $(1, 1, -1)$ of the original cube, there are fans of characteristics which at time t fill out all the points in the rectangle with corners $(1 + vt, 1 + vt(1 + \alpha), \pm[1 + t(1 + \alpha)])$ and $(1 + vt(1 + \alpha), 1 + vt, \pm[1 + t(1 + \alpha)])$, and similarly for the other eleven edges of the original cube. Finally, from the corner $(1, 1, 1)$, there is a fan of characteristics which at time t fills out the triangle with vertices $(1 + vt, 1 + vt(1 + \alpha), 1 + vt(1 + \alpha))$, $(1 + vt(1 + \alpha), 1 + vt, 1 + vt(1 + \alpha))$, $(1 + vt(1 + \alpha), 1 + vt(1 + \alpha), 1 + vt)$, with a similar statement holding for the other seven corners of the original cube.



(a)



(b)

Fig. 2. With the M_α of the text, the union of the characteristics emanating inward during shrinking from an original cube also have self-intersections and reentrant corners. (a) A (110) section (through the origin) of the points reached by these characteristics at time $t = 0.2$ is shown ($\alpha = 0.8$). (b) Multiple shocks form, leaving part of the "ears" in the combined form shown.

We note that there must be shocks emanating from the original corners and edges of the cube, whether $v = 1$ or $v = -1$, but the shocks are quite different in the two cases. When $v = 1$, the shock condition of stability to perturbation produces a single shock from each edge, cutting off all the “ears” and leaving a growing cube. But these characteristics are not cut off when $v = -1$. Rather, there are two shock surfaces emanating from each edge, allowing facets with normals such as $(1,1,0)$ to grow [with normal velocity $-(\sqrt{2 + \alpha}/\sqrt{2})$], and three shock surfaces emanating from each corner, allowing facets with normals $(\pm 1, \pm 1, \pm 1)$ to grow [with normal velocity $-(\sqrt{3 + 2\alpha}/\sqrt{3})$ and vertices such as $(1 - t(1 + \alpha), 1 - t(1 + \alpha), 1 - t)$]. Initially the shrinking form will be a combined form, shown in Fig. 2(b), with (100) , (110) and (111) facets; at later times the (100) will disappear first when the shock surfaces from different edges hit each other and form new shocks, and then the (110) facets will disappear when the shocks from different corners hit each other. The final form will be an octahedron.

4.2.2. Viscosity solution. We now show that for this M_α , the growing cube is a viscosity solution, but the shrinking cube is not.

For this level-set-of-a-function approach, the growing and shrinking cubes are given by the same functions u as in the isotropic case above, and so are the comparison functions ϕ . Again, the crucial test is with the linear comparison functions

$$\phi(\mathbf{x}, t) = 1 + vt - [ax_1 + bx_2 + (1 - a - b)x_3]$$

for any a, b with $0 < a < 1 - b < 1$, and with v being 1 in the growing case and -1 in the shrinking case. Again we have that for this ϕ , $u - \phi(\mathbf{x}, t) \leq 0$ for all (\mathbf{x}, t) . We compute that

$$\begin{aligned} \phi_t - M_\alpha(-\nabla\phi) &= 1 - \{(1 + \alpha) \\ &\times [a + b + (1 - a - b)] - \alpha a\} = -\alpha(1 - a) \leq 0 \end{aligned}$$

in the growing case and

$$\begin{aligned} \phi_t + M_\alpha(-\nabla\phi) &= -1 + (1 + \alpha) \\ &\times [a + b + (1 - a - b) - \alpha a] = \alpha(1 - a) \geq 0 \end{aligned}$$

in the shrinking case. Thus for this anisotropic velocity, the growing cube is a viscosity solution but the shrinking one is not, as is the case as determined by characteristics. [If one wishes to check that the comparison function

$$\phi(\mathbf{x}, t) = \varepsilon + v(t - t_0) + |\mathbf{x} - (x_{10} - \varepsilon, x_{20}, x_{30})|$$

(for $\varepsilon = \min\{1 + vt_0 - x_{20}, 1 + vt_0 - x_{30}\}$) satisfies the supersolution test, it is important to note that $\phi_t - M_\alpha(\nabla\phi)$ need be at least zero only at the single point (\mathbf{x}_0, t_0) , and it is indeed zero there.] Note that when $\alpha = 0$, M_α is convex, and both the growing and shrinking cubes are solutions, as determined either by the viscosity solutions here or the method of characteristics on the other PDE.

4.2.3. Crystalline method. The polyhedral growth model under the assumption that $\alpha = 0$ is particularly simple: W_∞ is a cube, no new facets are to be introduced, and facets simply translate at unit velocity (i.e. $ds_i/dt = 1$ or -1).

When α is non-zero, new facets of orientation $(1, 1, 0)$, $(-1, 1, 0)$, etc. are introduced along the appropriate edges and new facets of orientation $(1, 1, 1)$ etc. are introduced at the appropriate corners. When the velocity is positive (outward growth), these are cut off and do not appear in the surface. When the velocity is negative (inward growth, i.e. shrinking of the compact region), these new facets grow in size.

4.3. Saddle-shaped corners, isotropic normal growth ($\gamma \equiv 0$)

Now consider the saddle-shaped, re-entrant corner such as is formed by a box on a floor. For example, at time $t = 0$, let the corner be the union of the three planar pieces

$$\begin{aligned} \{(x_1, x_2, 0): \text{either } x_1 \geq 0 \text{ or } x_2 \geq 0\} \\ \{(x_1, 0, x_3): \text{both } x_1 \geq 0 \text{ and } x_3 \geq 0\} \\ \{(0, x_2, x_3): \text{both } x_2 \geq 0 \text{ and } x_3 \geq 0\}, \end{aligned}$$

oriented so that the normals are $(0, 0, 1)$, $(0, 1, 0)$ and $(1, 0, 0)$ respectively.

If the velocity is 1 on all normal directions, then this surface at a later time t is asserted to be the union of three planar pieces and a cylinder

$$\begin{aligned} [001] \\ \{(x_1, x_2, t): \text{either } x_1 \geq t \text{ or } x_2 \geq t \\ \text{or } [\text{both } x_1^2 + x_2^2 \geq t^2 \text{ and } \min(x_1, x_2)] \geq 0\} \end{aligned}$$

$$[010] \quad \{(x_1, t, x_3): x_1 \geq t, x_3 \geq t\}$$

$$[100] \quad \{(t, x_2, x_3): x_2 \geq t, x_3 \geq t\}$$

a $\langle 001 \rangle$ cylinder

$$\{(x_1, x_2, x_3): x_1^2 + x_2^2 = t^2, x_3 \geq t\}.$$

This surface is shown in Fig. 3.

4.3.1. Characteristics. With characteristics, one must introduce fans along all the slope discontinuities of the original surface, and there are shocks emanating from the points of slope discontinuity in the $x_3 = 0$ plane. The condition of earliest arrival of a characteristic determining when a point enters the crystal (and that once in it, it stays in it) is sufficient to determine the shock condition, since the isotropic mobility function is convex.

4.3.2. Viscosity solutions. We construct

$$u(\mathbf{x}, t) = t - \tau(\mathbf{x})$$

where $\tau(\mathbf{x})$ is the time t at which the point \mathbf{x} satisfies each of the above set of equations [in this case, $\tau(\mathbf{x})$ is also the distance from \mathbf{x} to the initial surface if \mathbf{x}

is in front of the surface, and the negative of that distance if \mathbf{x} is behind the surface]. Wherever this function u is smooth, which is on the set in space-time apart from the union of

$$\{(x_1, x_2, x_3, t): x_1 = t, x_2 \leq 0, x_3 = t\}$$

$$\{(x_1, x_2, x_3, t): x_1 \leq 0, x_2 = t, x_3 = t\}$$

$$\{(x_1, x_2, x_3, t): x_1^2 + x_2^2 = t^2, \min(x_1, x_2) \geq 0, x_3 = t\}$$

we know we can show that u passes both the sub-solution and the supersolution test. On that set where u has discontinuous first derivatives, one can use one linear function barrier from behind [$\phi(\mathbf{x}, t) = t - x_3$] plus cylindrical barriers from behind [one being $\phi(\mathbf{x}, t) = t - \sqrt{x_1^2 + x_2^2}$] to see that it must move at least that fast (i.e. u passes the supersolution test there). From in front, however, there are no functions which are suitable test functions in the definition, and therefore u automatically passes the subsolution test there.

4.4. Saddle-shaped corners, anisotropic normal growth ($\gamma \equiv 0$)

With the highly anisotropic velocity and non-convex M_x , we get a different type of growth. The surface at time t is asserted to be the union of the five planar pieces

[001]

$$\{(x_1, x_2, t): \text{either } x_1 \geq t(1 + \alpha) \text{ or } x_2 \geq t(1 + \alpha)\}$$

[010]

$$\{(x_1, t, x_3): x_1 \leq t \text{ and } x_3 \geq t(1 + \alpha)\}$$

[100]

$$\{(t, x_2, x_3): x_2 \leq t \text{ and } x_3 \geq t(1 + \alpha)\}$$

[101]

$$\{(x_1, x_2, x_3): x_1 + x_3 = t(2 + \alpha), x_1 \geq t, x_2 \geq t, x_2 \leq x_1\}$$

[011]

$$\{(x_1, x_2, x_3): x_2 + x_3 = t(2 + \alpha), x_2 \geq t, x_3 \geq t, x_1 \leq x_2\}$$

In particular, there is no [111] facet. This surface is shown in Fig. 4.

4.4.1. Characteristics. It is more difficult to see how to use characteristics for a saddle-shaped initial surface and a non-convex velocity function, in that it is not as obvious what the shock condition of stability to perturbation produces at the corner itself.

We see that there are characteristics from the vertical (convex) edge which cannot be used to construct a continuous solution and must be eliminated by the shock condition, and so the vertical edge continues to be just the intersection of [100] and [110] planes at distance t . Some of the characteristics along the horizontal (concave) edges do survive,

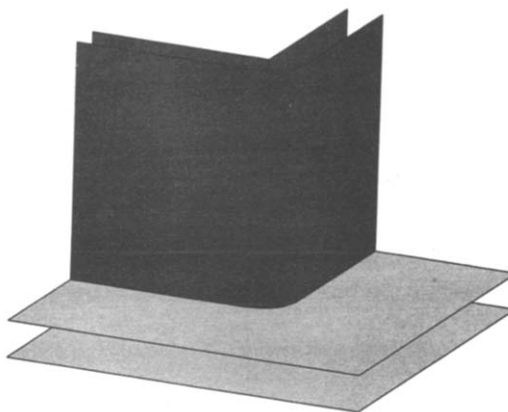


Fig. 3. During isotropic normal growth from a saddle-shaped corner, the corner disappears, the convex edge is rounded, while the concave edges remain sharp. The partially hidden surface is the initial corner; the surface in front is one after a period of growth.

producing growing facets of orientation [101] and [011] between the horizontal and vertical facets. At the corner itself, the “missing orientations” are all those in the open spherical triangle with vertices (1, 0, 0), (0, 1, 0), (0, 0, 1) and thus the fan of characteristics from the corner at time t fills out the triangle with vertices

$$t(1, 1 + \alpha, 1 + \alpha), t(1 + \alpha, 1, 1 + \alpha), t(1 + \alpha, 1 + \alpha, 1).$$

One of the edges of this triangle lies in the plane $x_3 = t$, but the points on the other two edges of the triangle connect to characteristics from the vertical edge which project beyond what can be connected to the growing vertical quarter-planes. Thus the triangular fan of characteristics from the corner contributes nothing, and the characteristics from the horizontal edges near the corner cross so that the result after the shock is that the [101] and [011] facets terminate at their intersection.

This is in fact the typical situation, as one can see perhaps more easily from the viscosity solution approach below: saddle-shaped corners where

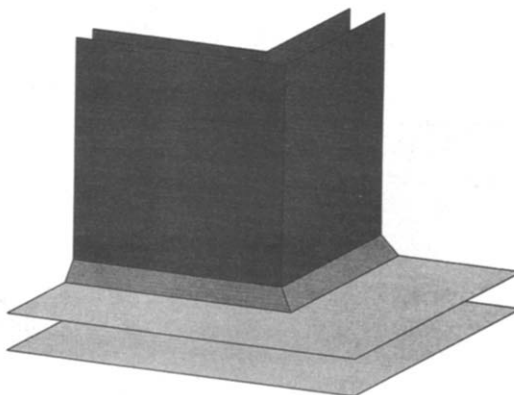


Fig. 4. During anisotropic normal growth, with the M_x of the text, from a saddle-shaped corner, the corner splits into two corners, the convex edge remains sharp, while the concave edges are truncated by (101) and (011) facets.

initially three facets meet produce no new orientations at the corners themselves on growth; instead, the evolving corner is that which results from intersections of the moving original surfaces and the new surfaces which can be shown to form along the edges through 2-d applications of characteristics.

4.4.2. Viscosity solutions. Again, we can use any families of smooth comparison surfaces from behind, except on the two non-horizontal lines of slope discontinuity, to show that u satisfies the supersolution test there, and families of smooth comparison surfaces from in front, except on the horizontal lines of discontinuity, to show it satisfies the subsolution test there. Again, on the excepted lines of slope discontinuity, the relevant test is satisfied automatically, since there are NO appropriate comparison functions.

Note in particular that there cannot be a plane segment in the (111) direction, since it would have to be in the plane containing $t(1 + 2\alpha/3)(1, 1, 1)$ (by barriers from both behind and in front), and the only point in that plane allowed by barriers from in front is the point $t(1 + \alpha, 1 + \alpha, 1)$ (which is in the surface). Also note that at each time $t > 0$ there is a point, $(t, t, t(1 + \alpha))$ with a saddle-shaped neighborhood, where four planar pieces meet. Comparisons cannot be made from either side at these points, and thus they automatically satisfy both the subsolution and the supersolution tests there.

4.4.3. Crystalline method. In the crystalline method with α positive, one again introduces extra facets at time 0, ones with normals $(1, 0, 1)$ and $(0, 1, 1)$ along the edges in the plane $x_3 = 0$ and one with normal $(1, 1, 0)$ along the vertical edge; one additionally adds a facet with normal $(1, 1, 1)$ at the origin (the initial distance of each of these facets is zero). Each facet is now translated with the appropriate velocity; the facet with normal $(1, 1, 0)$ is squeezed out and does not appear, but the facets with normals $(1, 0, 1)$ and $(0, 1, 1)$ grow. The facet with normal $(1, 1, 1)$ just fails to grow or be squeezed out, moving along right at the intersection point of the facets with normals $(0, 0, 1)$, $(1, 0, 1)$ and $(0, 1, 1)$.

4.5. Motion of a sphere by mean curvature ($\Omega \equiv 0$)

The sphere is a simple case where an explicit closed-form solution to the PDE with given initial data exists; other cases are rare.

4.5.1. Direct mapping. For motion of a sphere with initial radius r_0 by mean curvature, we can use method 1 (the direct mapping of a unit sphere) with $\mathbf{f}(\mathbf{x}, t) = r(t)\mathbf{x}$ for each \mathbf{x} in the unit sphere, to get the differential equation

$$dr/dt = -2/r$$

so that $r(t) = \sqrt{r_0^2 - 4t}$.

4.5.2. Viscosity solution. In the level-set-of-a-function approach, we can check that

$$u(\mathbf{x}, t) = r_0^2 - |\mathbf{x}|^2 - 4t$$

is a solution of the PDE

$$u_t = |\nabla u| \operatorname{div}(\nabla u / |\nabla u|)$$

with initial condition

$$u(\mathbf{x}, 0) = r_0^2 - |\mathbf{x}|^2$$

(which is 0 when $|\mathbf{x}| = r_0$). We see that $u = 0$ when $|\mathbf{x}| = \sqrt{r_0^2 - 4t}$, and so we get the same motion as for the direct method (as we must).

If instead we took the initial condition to be $w(\mathbf{x}, 0) = r_0 - |\mathbf{x}|$, which also is 0 when $|\mathbf{x}| = r_0$, then we can write $w = f(u)$ where $f(u) = r_0 - \sqrt{r_0^2 - u}$ can be found from the two different initial functions. Hence the solution would be $w(\mathbf{x}, t) = r_0 - \sqrt{4t + |\mathbf{x}|^2}$. It might be difficult to discover this solution w directly, but the solution u was found easily in this case by knowing that one seeks u as a function of $r = |\mathbf{x}|$ and t alone, and that $\nabla u / |\nabla u|$ will be $-\mathbf{x}/|\mathbf{x}|$, which has divergence $2/r$. The PDE thus becomes $u_t = |u_r|(-2/r) = 2u_r/r$, and the change of variables $s = r^2/4$ simplifies it further to $u_t = u_s$, with an obvious solution of $u = c - s - t = c - r^2/4 - t$ for some constant c and therefore with initial data $u(r, 0) = c - r^2/4$. Therefore c must be $r_0^2/4$, and other solutions can be found as above by finding the function that takes one initial data function into the other.

4.6. Motion of W by crystalline curvature ($\Omega \equiv 0$)

In the polyhedral case, if W is a polyhedron with each facet at unit distance from the origin [so that $\gamma(\mathbf{n}_i) = 1$ for each of the facet orientations], and if the initial surface is $r_0 W$, then the surface at time t under motion by crystalline weighted mean curvature (with mobility $M = 1$ on each facet) is just $\sqrt{r_0^2 - 4t} W$. If γ is not the same on each facet orientation, then W shrinks homothetically only if the mobility is proportional to γ [19].

We show this as follows. Suppose that there is a solution which is a scaled version of W , with scale factor $\rho(t)$. Then $s_i(t) = \rho(t)\gamma(\mathbf{n}_i)$, $\operatorname{Area}(S_i) = \rho(t)^2 \Lambda_i$, and $l_{ij} = \rho(t)L_{ij}$, where Λ_i is the area of the facet with normal \mathbf{n}_i in W and L_{ij} is the length of the edge in W between facets with normals \mathbf{n}_i and \mathbf{n}_j . We plug these values into the ODE for s_i

$$ds_i/dt = -M(\mathbf{n}_i) \frac{1}{\operatorname{Area}(S_i)} \sum_j \delta_{ij} f_i l_{ij}$$

and obtain

$$\gamma(\mathbf{n}_i) d\rho(t)/dt = -[1/\rho(t)]M(\mathbf{n}_i) \frac{1}{\Lambda_i} \sum_j f_i L_{ij}$$

which says

$$\begin{aligned} (1/2)d\rho^2/dt &= -[M(\mathbf{n}_i)/\gamma(\mathbf{n}_i)](1/\Lambda_i) \sum_j f_i L_{ij} \\ &= -2M(\mathbf{n}_i)/\gamma(\mathbf{n}_i). \end{aligned}$$

The left-hand side does not depend on i , and therefore, in order for this scaled solution to exist, it is necessary and sufficient that $M(\mathbf{n}_i)/\gamma(\mathbf{n}_i)$ not depend

on i —i.e. that M be proportional to γ . If we assume that $M = \gamma$ (which is the case in particular when γ and M are both 1 on each facet of W), then the equation above has the solution

$$\rho(t) = \sqrt{r_0^2 - 4t}.$$

We have thus found one solution to the system of ODE with the given initial conditions, and by uniqueness it is the only one.

Note that when γ is 1 on every facet, W itself is circumscribed about a unit sphere, and W moving by weighted mean curvature remains circumscribed about that sphere moving by mean curvature. This is true for any W whose facets are all unit distance from the origin, whether regular polyhedra or not. The sphere is in fact a special case of W shrinking homothetically, since the surface of the Wulff shape for the function which is 1 on every unit vector is the unit sphere.

If we wished to approximate motion of a sphere by mean curvature by motion by crystalline curvature, we could take W to be a polyhedral approximation to a sphere, with each facet at distance 1 from the origin. We could then circumscribe W itself about the unit sphere, and put a scaled version of W inside the unit sphere. The smaller version would shrink more rapidly (and not stay inscribed, if it were originally), but by choosing closer and closer approximations to the sphere, one could make the factor r_0^2 be as close to 1 as we wish, and therefore have the distance between the inscribed and circumscribed polyhedra stay as small as we wish.

4.7. Motion of a figure-8 by weighted mean curvature ($\Omega \equiv 0$)

This is an example of a configuration with a self-intersection where four curves meet. There is not one unique motion by weighted mean curvature for this curve; rather, the motion depends on how the set of points is interpreted. Different methods interpret the intersection point differently and give different results. Thus this curve is representative of the only cases known in which different results are known to arise when different methods apply.

4.7.1. Crystalline approach (and other mapping approaches). In this approach, which evolution occurs depends on how the curve is presented. If it is presented as two curves happening to overlap on one point, the curves shrink independently [Fig. 5(b)]. If it is presented as one draws a figure-8, so that one loop has a counterclockwise orientation and the other a clockwise orientation, it evolves as a figure-8 until it shrinks the smaller loop to zero; it then adds an infinitesimal segment at the resulting sharp corner, moves it rapidly, and shrinks the remaining loop [Fig. 5(d)]. If it is presented as one large curve pinched together in the middle, then the pinches straighten out, the curve becomes convex, and finishes by shrinking to a point [Fig. 5(a)]. If it is presented as two overlapping triple points, then it separates

the triple points and shrinks as a double-bubble [Fig. 5(c)], as seen in a video [18].

In addition Fig. 5 demonstrates some other aspects of motion by crystalline curvature. Here W is a regular octagon, while the initial shape is a joining of two hexagons (for no reason other than the choice of the authors; the choice of octagonal initial shapes might be more “natural,” given the octagonal Wulff shape, but it would illustrate fewer properties of crystalline motion). The two horizontal sides of each hexagon are parallel to facets of the Wulff shape; all other sides are not parallel to facets of the Wulff shape and they immediately become varifolds. (The fact that they are varifolds is not apparent in the figure, since they are drawn as actual varifolds rather than as finite-scale corrugations approximating varifolds.) The remaining facets of the octagons appear immediately at all corners and begin moving [the crossing in Fig. 5(d) is not a corner]. Note that the varifolds don’t move; they have zero weighted curvature. The varifolds shrink rapidly to zero length by the encroachment of the adjoining octagonal facets; it is the octagonal facets which move. Note in Fig. 5(a) that the velocities of the horizontal facets on the right drop to zero when the varifolds on their left are consumed. These facets then are bounded by a regular and inverse corner and have zero crystalline curvature. The facets to the left of these facets stop moving for the same reason. Note also the abrupt changes in velocities of the facets neighboring the right horizontal facets when these horizontal facets have shrunk to zero. The inverse corner disappears, the facets merge and their lengths are combined. Crystalline curvature, and hence velocity, is inversely proportional to the length of a facet. Rather crude numerical techniques are used to handle the infinite velocities at which the inserted octagonal facets initially move; this is the source of the lack of mirror symmetry in Fig. 5.

4.7.2. Brakke’s varifold approach (isotropic). In this approach, the solution is non-unique, but each possible solution evolves as a one-dimensional varifold. The evolutions probably include all physically reasonable evolutions with the given initial data.

4.7.3. Viscosity-solution approach (isotropic). In this approach, the zero-level set becomes 2-dimensional rather than remaining a 1-dimensional curve [7]. Evans and Spruck conjectured [7] that the isotropic analogues of all of the above possible evolutions, and switches from one to another at times after 0, are contained in this evolving 2-dimensional zero-level set. It appears that the varying interpretations in the mapping approach (which reflect sensitive dependence on initial conditions) give rise to this non-physical behavior in the viscosity solution approach. If one tries to apply the level-set method to the case where there are triple junctions, a similar non-physical spreading out of the interface to a whole region always occurs [Fig. 5(e)], and this cannot be removed by perturbation.

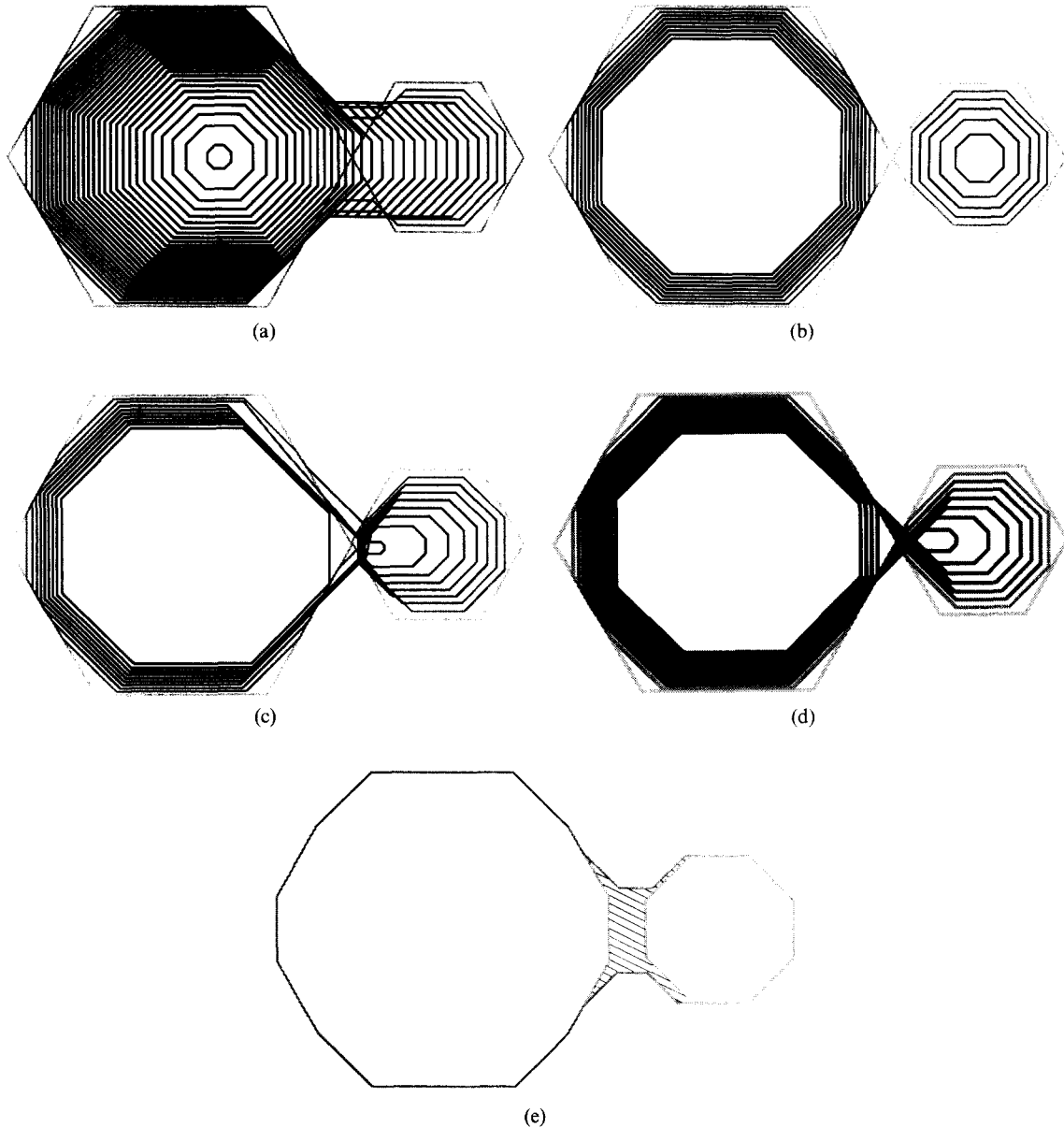


Fig. 5. The results for motion by crystalline curvature from an initial figure-8 depend on how the initial shape is interpreted. Curves are drawn at equal time intervals with earlier times shown lighter; in the first figure, the entire evolution is shown, while in the others, only the early times are presented. In all cases shown, both W and W_∞ are regular octagons. (a) If the 8 is presented as one large curve pinched together in the middle, then the pinch straightens out, resulting in a single curve which then shrinks to zero. (b) If the 8 is presented as two curves contacting at one point, two curves result, and they shrink independently, with the smaller one disappearing first. (c) If the 8 is presented as two overlapping triple points, then the triple points separate, giving two shrinking bubbles, that, depending on the angle at the crossing, will contact along the line between the triple junctions as shown or be strung together by that line. (d) If the 8 is presented as an immersion, remaining a figure 8 until the smaller loop shrinks to zero size. (e) In the viscosity solution approach, the set where $u=0$ at any small time $t > 0$ becomes 2-dimensional and thus non-physical; if it applied in the crystalline context, the result at some small time $t > 0$ would probably be as indicated, with the hatched region (and a very thin extension around each bulb) being the set on which $u=0$.

5. COMPUTATIONAL VERSIONS OF THESE METHODS AND COMPARISONS

The relationships discussed in this section are summarized in Table 2.

5.1. 2-d, no triple junctions

For the motion of closed curves in 2-d moving by prescribed velocity, curvature, or the general geometric growth law, there have been many programs

Table 2. Computation

Method	Who	2-d	3-d	γ	M	Ω^a	Multiple grains?	Topological changes?
Mapping	Brakke—Evolver	✓	✓	Isotropic or crystalline ^c	Isotropic	0	Yes	“By hand” ^b
	Frost	✓		Isotropic	Isotropic	0	Yes	Automatic
Crystalline	Dziuk		✓	Isotropic	Isotropic	0	No	No
	Taylor	✓		Crystalline	Any compatible with γ	c	Yes	Automatic
	Taylor		✓ ^c	Crystalline	Any compatible with γ	c	No ^d	Automatic ^c
Viscosity	Osher & Sethian	✓	✓	Isotropic	Isotropic	c	No	Automatic
Phase field	Osher & Bence	✓		0	Isotropic	c	Yes	Automatic
	With diffusion—Kobayashi	✓	✓	Anisotropy via ε	Some anisotropy	0	No	Automatic
Q -State Potts	Anderson, Srolovitz, Grest, etc.	✓	✓ ^c	Determined	Isotropic	0	Yes	Automatic

^ac = constant, with different constants for different interfaces when treating multiple grains.

^bAutomatic in 2-d.

^cPartial.

^dBelieve that these restrictions are not essential to the method.

written, and all of the methods except Brakke’s varifold, least time, and regularization have been used.

The direct mapping method consists of putting points along an initial curve, moving them in the normal direction the appropriate distance, and (typically) interpolating a smooth curve between the points. Such a method makes it quite difficult to handle the shocks that can develop in motion by prescribed velocity, and orientation and especially curvature are sensitive to the type of interpolation used. Computational problems in such motion include deciding when to add or delete points along the interface, and detecting and making topological changes. Nevertheless, this is the most convenient way to model moving interfaces up to times when it fails (due to these computational problems becoming essentially insurmountable). A variation used by Brakke [93], for motion by curvature or weighted curvature, is to do piecewise linear interpolation, and compute the curvature by determining how the area enclosed and curve length change with changes in position of the vertices, using the idea that the curvature is the change in length with regard to area under deformations.

Using characteristics to calculate motion by a prescribed function of the normal direction has much in common with the direct mapping method; here, one just goes in the direction appropriate to the characteristic, rather than in the normal direction. The normals are known at the points (since normals stay constant on characteristics when v is independent of x , and otherwise are a known function of position), so the interpolation scheme can utilize that information; curvature information is not needed. There are still problems with finding and tracking shocks, with detecting and making topological changes, with increasing or decreasing the number of nodes along the curve, and so forth. But when these problems have known solutions, programs can be written; for example, Carter and Handwerker [122] wrote a

program to compute curves by following characteristics to obtain the figures contained in our previous paper [2], but those were very special cases where the position of the shocks was known by symmetry.

The formulation in terms of finding level sets of viscosity solutions to degenerate elliptic equations was designed precisely to avoid these problems posed by trying to compute with characteristics [6]. It also avoids the problem of trying to measure the normal and curvature of an interpolated surface. There is, however, a large computational overhead caused by having to compute u everywhere, when you only want to know where $u = 0$.

It works well for curves provided the initial curve has no self-intersections; at self-intersection points, it produces physically unrealistic results. The unrealistic results at triple-junction-type intersection points are unavoidable in the current formulation, because the method is designed to find curves separating two phases. To model situations as in Fig. 5(a, b) (but with smooth curves), giving the initial data a slight perturbation will resolve its dilemma and put it back in the situation of moving curves without self-intersections.

The crystalline method is naturally amenable to computation, and has been implemented in a program by Taylor [17, 18] and, independently (and in a more limited setting) by Roberts [96]. In this method, the motion law can have both γ and Ω nonzero, or one or the other zero; as stated above, γ and M are given on the same finite collection of normal directions. The initial curve must be polygonal. (A smooth initial curve might be approximated by a polygonal curve.) The program stores the normal directions, distances from the origin, and adjacencies of the line segments and changes the distances in accord with the system of ODE. Initial adjacencies are checked to see if they agree with those in \mathcal{W} , and if not, the proper adjacencies are filled in. Line segments that become of zero length are deleted, and the adjacent line segments are merged if they

have the same direction and otherwise the proper adjacencies, as determined by W , are filled in. Triple junctions and the varifolds they tend to leave behind in their motion are handled by using the variational formulation, and by introducing new line segments at each time step as needed.

A 2-state Potts model [method (9)] could be used to model motion by curvature, but as has been stated before, just what continuum model this lattice model approximates is unclear, and careful studies of the evolution of simple initial bodies like squares is only now being undertaken [Anderson, personal communication].

The phase field approach has had limited use computationally for motion by curvature; it is usually used for the problem when diffusion fields must also be solved for, as in dendritic crystal growth [25, 112]. Osher [110] has compared the use of the phase field method with that of level sets of viscosity solutions and concluded that Δx must be quite small in comparison to ε for the phase field method to yield reasonable computational results.

5.2. 2-d multigrain or multiphase

The direct mapping method in the multi-grain case for motion by curvature has been treated computationally by both Brakke [93] and Frost [95]; Brakke's evolver program has many additional bells and whistles, such as allowing γ to be a function of \mathbf{n} and including body forces like gravity, but his program is designed to be run interactively, and must be assisted through steps involving changes of topology, insertion or deletion of vertices, etc. (see *Note added in proof*). Frost's programs are designed to run large simulations of 2-d grain growth, and run in a "hands-off" fashion, recording certain types of data as the simulation progresses. Here the motion is done in two steps, moving points on the interior of the curves and then moving the triple junctions to restore 120° angles.

The Q -state Potts model has been used to model many types of 2-d grain growth, on different types of lattices, with different (constant) values of surface energy for different types of interfaces, with fixed obstacles, etc. [59, 60, 113]. It is difficult, however, to determine what the effect of the lattice is, and it is not clear that it really models motion by curvature. Nevertheless, this method has been developed to the point where it is used to investigate many features of grain growth.

The crystalline method also has been implemented for multiple grains (and with possible different γ and M for different interfaces) [17, 18].

Osher and Bence [110] are just developing computational methods which handle a triple junction. They replace the single indirect PDE by a pair of equations, and define the interface to be the union of the zero sets of the two functions. They have applied it only to the case of constant normal motion ($\gamma = 0$), with different constants for different interfaces.

We know of no case where motion of multiple grains has been done computationally using a phase field motion.

Taylor [15] showed how to use characteristics to do motion of multiple grains, but did not implement this method computationally, due to the usual problem with finding and tracking shocks and of detecting when topological changes should be made.

5.3. 3-d

Brakke has a full-featured program called *evolver* for computing solutions to variational problems, including those with free boundaries, prescribed volumes, multiple grains with grain junctions, etc., and the program is in the public domain with a good reference manual [93]. One of its options is a motion-by-mean-curvature mode. This program is designed to be run interactively, so the operator must assist it through changes of topology, addition and deletion of vertices, etc. (see *Note added in proof*). Also, the motion by curvature runs best when the triangles of the surface triangulation are of approximately the same size. Again, there is no proof of how well it actually approximates motion by curvature.

Dziuk [94] has a program for moving parametrized surfaces by curvature (in the mapping approach), together with some error bounds. However, it cannot handle anything but motion of smooth surfaces, and it cannot make topological changes. (Hoffman [123] primarily computes minimal surfaces, typically using the Weierstrass representation, and does not do motion problems.)

Some Monte Carlo simulations have been done in 3-d (T. Rollet, personal communication). We have heard that there is a problem with getting things to move with some lattices (M. P. Anderson, personal communication). The curse of dimensionality (too long computational time) also strikes here.

An unusual method is the Voronoi-cell evolver method described by Almgren [124]. It probably does do some approximation to motion by curvature or weighted mean curvature.

Motion in 3-d by weighted mean curvature for the crystalline case is under development [18]. A preliminary program has been successfully applied to initial surfaces on a fixed boundary that satisfy some rather restrictive conditions. The program does not yet handle triple junctions.

6. DISCUSSION

We see the following as being important open problems. First, there are these open mathematical problems:

- Extending all the methods, theoretically and computationally, to multiple grain or phase junctions.
- Developing any method to be a good 3-d computational tool, especially with multiple grains.
- Proving that the computational schemes stay close to the theoretical solutions.

- Proving results for arbitrary γ , especially in 3-d.
- Putting anisotropy in γ and M into the phase field method (in a natural way).
- Extending the phase field method to vector-valued u (probably necessary for multiple phases and grains).
- Extending the viscosity solution method to non-smooth and non-strictly-convex γ .
- Exploring whether the viscosity solution is really the physically correct one for non-convex M .
- Determining whether a viscosity solution can develop an interior for some times $t > t_0 > 0$ if it does not have an interior for $0 \leq t \leq t_0$. This should be related to uniqueness questions for physically realistic motions.
- Determining whether the viscosity solution can ever develop an interior if Ω is non-zero.
- Extending the viscosity solution method to vector-values u (necessary for multiple grains).
- Extending viscosity-solution results to discontinuous dependence on position.
- Understanding what continuum model is the limit of the Q -state Potts model, and what behavior the Monte Carlo scheme exhibits, in both 2-d and 3-d.
- Extending the crystalline model to all polyhedral 3-d surfaces and to multiple grains in 3-d.
- Developing a better description of which characteristics must be eliminated at shocks originating at saddle-shaped corners of an initial surface for non-convex M ($\gamma \equiv 0$), and extending the method of characteristics and minimax time formulation for non-convex M to multiple phases.

All the methods have stringent requirements on when they can be applied; the following open problems deal with the question: when can you use them as an approximation to the real world where the conditions may not be met?

- Determining the nature of the convergence of solutions with $\gamma > 0$ to solutions with $\gamma \equiv 0$ (so that materials scientists can know when they can reliably neglect surface energy and use, for example, characteristics to get simple solutions “by hand”) [125].
- Determining the nature of the convergence of solutions as a function of γ . In particular, determining the nature of such convergence when crystalline γ are used to approximate arbitrary γ .
- Determining the validity of using a sharp interface model for a diffuse interface and vice versa (recent work [111]) goes far toward giving a positive answer to this in one case, as mentioned in 2.8 above).

Several of the nine methods outlined in Section 2 have a parallel formulation when there is an additional diffusion field in the problem, and these methods are being pursued theoretically and computationally. These include the mapping method [126–131], the phase field method [25–28, 112, 132],

the viscosity-solution method [133–135], and the crystalline method [136].

- Extending further both theory and computation, for various methods, to the case where there is diffusion.

- Determining when mass and/or heat flow can be neglected, and the nature of the convergence of solutions when heat and/or mass flow are not neglected to those where they are neglected.

The mathematics requires quite precise formulations of the problem, and different statements can give quite different results for motion from corners and edges. All are correct from a mathematical point of view, but determining what is correct from a materials science point of view requires experiment and physical theory.

- Determining experimentally when the framework of geometric crystal growth is applicable, and what determines M . Does the equation we have been using adequately describe v ? In essence, one measures v and γ and deduces M . For example, in domain growth near a second-order transition, $\Omega = 0$, γ is isotropic and goes to 0 at the critical temperature, but v is independent of temperature and orientation [36]; thus M has to go to infinity as a function of temperature in this formulation (while remaining isotropic), even though individual atoms have finite diffusion rates.

- Determining what physically realistic conditions to apply when there are corners in the crystal shape [e.g. is stability the right criterion for characteristics, and is the viscosity solution the right one? When might other criteria be appropriate? See the discussion at the end of method (1) in Section 2.]

- Determining whether or not γ is convex. It is not obvious how one would measure γ for the missing orientations of W , or even whether a surface could have a missing orientation whose energy would be higher than that if γ were convex, since (in the absence of an extra energy due to edges) decomposition into a varifold would result in an instantaneous surface energy drop. One might be able to deduce the answer from the expected behavior of a nonconvex γ . For example, some orientations that are not in W may be metastable; they are stable with respect to small undulations but unstable with respect to finite orientation changes as in a varifold [58].

- Resolving experimentally questions raised by differences in the formulations of the problem and in solutions. The mathematics required that certain assumptions be made explicit about what happens physically at edges and corners. Which of the different assumptions in this paper are physically realistic is a question that requires an answer from experiment or from physical theory.

Acknowledgements—Conversations with Robert Kohn and L. Craig Evans were extremely useful in the preparation of this paper. The authors gratefully acknowledge the partial support from NIST, MSRI, ONR, NSF, AFOSR and DARPA.

Note added in proof—Progress continues to be made at a rapid pace, both in computation and theory. Much of this is outlined in the publication *Computational Crystal Growers Workshop* (edited by J. E. Taylor), Selected Lectures in Mathematics, Am. Math. Soc. (Providence) 1992, in press. It consists of 29 short papers and an 80-minute videotape containing 14 submitted videos, nearly all relevant to this overview. Some notable features are:

(1) Merriman, Bence and Osher have developed a variant of the phase field method for motion by mean curvature and some other geometric motions. It can handle multiple phases and is expected to work computationally in 3-d as well as in 2-d. It alternates a step of convoluting the characteristic functions of sets with the heat kernel (or some other smoothing function) with a step of rounding the resulting smoothed functions back to characteristic functions.

(2) Brakke's evolver program now runs in 2-d in a "hands-off" fashion, needing no assistance in changing topology, inserting and deleting vertices, etc. The manual is available, as GCG 31, from the Geometry Center, University of Minnesota, 1300 South Second Street, Minneapolis, MN 55415, U.S.A. The program plus manual is also available by anonymous ftp to geom.umn.edu, as the file pub/evolver.tar.Z.

(3) Taylor's crystalline program in 3-d has been expanded to deal with surfaces without boundaries and some simple topological changes. Mobilities and driving forces Ω which depend on position and shape, such as in an imposed temperature gradient, can be treated. The facet-splitting process is better understood and implemented.

(4) Programs for computing dendritic crystal growth are able to reproduce many experimentally observed phenomena (papers and videos by R. Almgren, Kobayashi and Roosen; papers by Dziuk and by Bänsch and Schmidt).

(5) Ilmanen has proven the convergence of the Allen-Cahn equation to Brakke's motion by mean curvature, in a preprint of that title. This preprint is summarized in the proceedings.

(6) F. Almgren, Taylor and Wang have put a firm theoretical base under the optimization approach.

REFERENCES

1. Y.-G. Chen, Y. Giga and S. Goto, *J. diff. Geometry* **33**, 749–786 (1991).
2. J. W. Cahn, J. E. Taylor and C. A. Handwerker, in *Sir Charles Frank, OBE, FRS, An eightieth birthday tribute* (edited by R. G. Chambers, J. E. Enderby, A. Keller, A. R. Lang and J. W. Steeds), p. 88–118. Hilger, New York (1991).
3. K. A. Brakke, *Math. Notes*, Princeton Univ. Press, Princeton, N.J. (1978).
4. J. A. Sethian, *Commun. math. Phys.* **101**, 487 (1985).
5. J. A. Sethian, *J. diff. Geometry* **31**, 131 (1990).
6. S. Osher and J. A. Sethian, *J. Comput. Phys.* **79**, 12 (1988).
7. L. C. Evans and J. Spruck, *J. diff. Geometry* **33**, 635 (1991).
8. L. C. Evans and J. Spruck, *Trans. Am. Math. Soc.*, in press.
9. L. C. Evans and J. Spruck, Motion of level sets by mean curvature III, to be published.
10. M. G. Crandall, L. C. Evans and P. L. Lions, *Trans. AMS* **487** (1984).
11. H. M. Soner, *J. diff. Equations*, to be published.
12. S. Angenent and M. E. Gurtin, *Arch. ration. Mech. Analysis* **108**, 323 (1989).
13. M. Gurtin, *Arch. ration. Mech. Analysis* **100**, 275 (1988).
14. M. Gurtin, Thermomechanics of evolving phase boundaries in the plane. Oxford Univ. Press.
15. J. E. Taylor, The motion of multiple phase junctions under prescribed phase-boundary velocities, to be published.
16. J. E. Taylor, *Crystals, In Equilibrium And Otherwise*, Selected Lectures in Mathematics, Am. Math. Soc. (1989).
17. J. E. Taylor, *Proc. Symp. in Pure Math*, in press. (Research report GCG26, Geometry Supercomputer Project, University of Minnesota.)
18. J. E. Taylor, in *Computing Optimal Geometries* (edited by J. E. Taylor), Selected Lectures in Mathematics, Am. Math. Soc. (1991).
19. J. E. Taylor, In *Differential Geometry*, A symposium in honour of Manfredo do Carmo (edited by B. Lawson and K. Tenenblat), pp. 321–336. Longman, Essex (1991).
20. *Computing Optimal Geometries* (edited by J. E. Taylor), Selected Lectures in Mathematics, Am. Math. Soc. (1991). (This publication, which is accompanied by a videotape, has extended abstracts and video clips for many methods of crystal growth and other shape problems.)
21. L. Bronsard and R. Kohn, *Commun. pure appl. Math.* **4**, 983 (1990).
22. L. Bronsard and R. V. Kohn, *J. diff. Equations* **90**, 211 (1991).
23. J. Rubenstein, J. Sternberg and J. B. Keller, *SIAM J. appl. Math.* **49**, 1722 (1989).
24. J. Rubenstein, P. Sternberg and J. B. Keller, *SIAM J. appl. Math.* **49**, 116 (1989).
25. G. Caginalp, in *Nonlinear systems of partial differential equations in applied mathematics, Part 2* (Santa Fe, N.M., 1984), pp. 347–369, Lectures in Appl. Math., 23, Amer. Math. Soc., Providence, R.I. (1986).
26. G. Caginalp, in *Material instabilities in continuum mechanics (Edinburgh, 1985–1986)*, pp. 35–52. Oxford Univ. Press, New York (1988).
27. G. Caginalp, *Phys. Rev. A* **39**, 5887 (1989).
28. G. Caginalp, *IMA J. appl. Math.* **44**, 77 (1990).
29. M. Bardi and S. Osher, *SIAM J. Analysis* **22**, 344 (1991).
30. G. Barles, L. Bronsard and P. E. Souganidis, Front Propagation for reaction diffusion equations of bistable type, Ann. Inst. H. Poincaré, Analyse Non-linearie, to be published.
31. P. de Mottoni and M. Schatzman, *C.R.A.S.* **309**, 453 (1989).
32. P. de Mottoni and M. Schatzman, Development of interfaces in R^N , to be published.
33. S. J. Altschuler, S. B. Angenent and Y. G. Giga, Hokkaido U. Preprint Series # 130 Dec. (1991).
34. J. E. Taylor, *Acta metall.* **40**, 1475 (1992).
35. J. W. Christian, *The theory of transformations in metals and alloys*, 2nd edn, Part I, Section 53, pp. 476–482. Pergamon Press, Oxford (1975).
36. S. M. Allen and J. W. Cahn, *Acta metall.* **27**, 1085 (1979).
37. J. W. Cahn and S. M. Allen, *J. Physique* **38**, C7-51 (1977).
38. G. Wulff, *Z. Kristallogr.* **34**, 449 (1901).
39. R. Gross, Abhandl. d. K. Sachsische Gesellsch. d. Wissensch., math.-phys. Kl. XXXV, iv. 12, pp. 137–202 (1918).
40. F. C. Frank, in *Growth and Perfection of Crystals* (edited by R. H. Doremus, B. W. Roberts and D. Turnbull), pp. 411–419. Wiley, New York (1958).
41. F. C. Frank, *Metal Surfaces*, pp. 1–15. Am. Soc. Metals, Metals Park, Ohio (1963).
42. F. C. Frank, *Z. phys. Chem. N.F.* **77**, 84 (1972).
43. A. A. Chernov, *Soviet Phys. Crystallogr.* **7**, 728 (1963).
44. A. A. Chernov, *Modern Crystallography III, Crystal Growth*, p. 219. Springer, Berlin (1984).

45. W. K. Burton, N. Cabrera and F. C. Frank, *Phil. Trans. R. Soc. A* **243**, 299 (1951).
46. R. C. Brower, D. A. Kessler, J. Koplik and H. Levine, *Phys. Rev. Lett.* **51**, 1111 (1983).
47. M. D. Kruskal and H. Segur, *Stud. appl. Math.* **85**, 129 (1991).
48. W. B. Hillig, *Acta metall.* **14**, 1868 (1966).
49. P. R. Pennington, S. F. Ravitz and G. J. Abbaschian, *Acta metall.* **18**, 943 (1970).
50. G. J. Abbaschian and S. F. Ravitz, *J. Cryst. Growth* **44**, 453 (1978).
51. D. J. Barber, F. C. Frank, M. Moss, J. W. Steeds and I. S. T. Tsong, *J. Mater. Sci.* **8**, 1030 (1973).
52. M. J. Nobes, I. V. Katardjiev, G. Carter and R. Smith, *J. Phys. D: Appl. Phys.* **20**, 870 (1987).
53. G. Carter, I. V. Katardjiev and M. J. Nobes, *Phil. Mag.* In press.
54. J. D. Livingston and J. W. Cahn, *Acta metall.* **22**, 495 (1974).
55. C. S. Smith, in *Metal Interfaces*, p. 65. Am. Soc. Metals, Metals Park, Ohio (1952).
56. J. von Neumann, discussion to Ref. [55], in *Metal Interfaces*, p. 65. Am. Soc. Metals, Metals Park, Ohio (1952).
57. W. W. Mullins, *J. appl. Phys.* **27**, 900 (1956).
58. W. W. Mullins, *Metal Surfaces*, pp. 44–45. Am. Soc. Metals, Metals Park, Ohio (1963).
59. M. P. Anderson, D. J. Srolovitz, G. S. Grest and P. S. Sahni, *Acta metall.* **32**, 783 (1984).
60. D. J. Srolovitz, G. S. Grest, M. P. Anderson and A. D. Rollett, *Acta metall.* **36**, 2115 (1988).
61. J. W. Cahn, *Acta metall. mater.* **39**, 2189 (1991).
62. C. A. Handwerker, J. W. Cahn, D. N. Yoon and J. E. Blendell, in *Diffusion in Solids: Recent Developments* (edited by M. A. Dayananda and G. E. Murch), pp. 275–292. The Metallurgical Society (1985).
63. D. N. Yoon, J. W. Cahn, C. A. Handwerker, J. E. Blendell and Y. L. Baik, *International symposium on interface migration and control of microstructure*, pp. 1–13. Am. Soc. Metals, Metals Park, Ohio (1986).
64. C. A. Handwerker, *Diffusion Phenomena in Thin Films and Microelectronic Materials* (edited by D. Gupta and P. S. Ho), pp. 245–322. Noyes Publications, Park Ridge, N.J. (1988).
65. J. P. Hirth and J. Lothe, *Theory of Dislocations*. Wiley, New York (1982).
66. M. Peach and J. S. Koehler, *Phys. Rev.* **80**, 436 (1950).
67. F. R. N. Nabarro, *Adv. Phys.* **1**, 269 (1952).
68. J. W. Cahn, *Acta metall.* **11**, 1275 (1963).
69. M. Kato, T. Mori and L. H. Schwartz, *Acta metall.* **28**, 285 (1980).
70. L. H. Schwartz, in *Modulated Structure Materials* (edited by T. Tsakalagos), pp. 411–423. NATO/ASI Series, Nijhoff (1984).
71. T. Surek, S. R. Coriell and B. Chalmers, *J. Cryst. Growth* **50**, 21 (1980).
72. T. Surek, *Scripta metall.* **10**, 425 (1976).
73. J. D. T. J. Hurler, *Adv. Colloid Interface Sci.* **15**, 101 (1981).
74. J. W. Gibbs, *Collected Works*, Vol. 1, p. 104, p. 257. Longman Green (1928).
75. D. Dinghas, *Z. Kristallogr.* **105**, 304 (1944).
76. H. Busemann, *Am. J. Math.* **71**, 743 (1949).
77. R. T. Rockafellar, *Convex Analysis*. Princeton Univ. Press, Princeton (1970).
78. R. T. Rockafellar, *The Theory of Subgradients and its Applications to Problems of Optimization. Convex and Nonconvex Functions*. Heldermann Verlag, Berlin (1981).
79. D. W. Hoffman and J. W. Cahn, *Surf. Sci.* **31**, 368 (1972).
80. J. W. Cahn and D. W. Hoffman, *Acta metall.* **22**, 1205 (1974).
81. M. Gage and R. Hamilton, *J. diff. Geometry* **23**, 285 (1986).
82. M. Gage, *Inventiones Math.* **76**, 357 (1984).
83. M. Gage, Curve Shortening in Relative Geometries, Preliminary report.
84. M. Grayson, *J. diff. Geometry* **26**, 285 (1987).
85. G. Huisken, *J. diff. Geometry* **20**, 237 (1984).
86. G. Huisken, *J. diff. Geometry* **31**, 285 (1990).
87. K. Ecker and G. Huisken, *Ann. Math.* **130**, 453 (1989).
88. K. Ecker, *Math. Zeit.* **180**, 179 (1982).
89. J. Hass and P. Scott, Shortening curves on surfaces, to be published.
90. S. Angenent, *Ann. Math.* **132**, 451 (1990).
91. S. Angenent, *Ann. Math.* **133**, 171 (1991).
92. O. A. Ladyzhenskaya, V. A. Solonikov and N. N. Ural'ceva, *Linear and Quasi-linear Equations of Parabolic Type*, Transl. Math. Monographs 23 AMS (1968).
93. K. A. Brakke, Evolver program, Surface Evolver Manual, Research Report GCG 31, The Geometry Center, Univ. Minn. (see *Notes added in proof*).
94. G. Dziuk, An algorithm for evolutionary surfaces, Sonderforschungsbereich 256, report no. 5, Bonn.
95. H. J. Frost and C. V. Thompson, *J. Electron. Mater.* **17**, 447 (1988).
96. S. Roberts, A line element algorithm for curve flow problems in the plane, CMA Research Report 58, Australian National University (1989).
97. M. A. Grayson, *Duke Math. J.* **58**, 555 (1989).
98. W. K. Allard, *Ann. Math.* **95**, 417 (1972).
99. L. C. Evans and P. E. Souganidis, *Indiana Univ. Math. J.* **33**, 773 (1984).
100. P. M. Morse and H. Feshbach, *Methods of Theoretical Physics*, p. 847. McGraw Hill, New York (1953).
101. F. John, *Partial Differential Equations*, 2nd edn, pp. 38–40. Springer, New York (1975).
102. R. Haberman, *Mathematical Models*. Prentice-Hall, Englewood Cliffs, N.J. (1977). (Pages 257–394 deal with traffic flow, through the use of characteristics with shocks and fans.)
103. P. L. Lions, *Generalized Solutions of Hamilton-Jacobi Equations*. Pitman, London (1982).
104. T. Ilmanen, The level-set flow on a manifold, *Proc. Symp. in Pure Math.*, in press.
105. Y. Giga and S. Goto, *J. Math. Soc. Japan*. in press.
106. M. G. Crandall, H. Ishii and P. L. Lions, *Bull. Am. Math. Soc.*, in press.
107. Y. Giga, S. Goto, H. Ishii and M.-H. Sato, *Indiana Univ. Math. J.* **40**, 443 (1991).
108. T. Ohta, D. Jasnow and K. Kawasaki, *Phys. Rev. Lett.* **49**, 1223 (1982).
109. Y.-G. Chen, Y. Giga and S. Goto, *Proc. meeting on Functional Analysis and Related Topics* (edited by S. Koshi) Sapporo (1990).
110. S. Osher, in *Computing Optimal Geometries* (edited by J. E. Taylor) Selected Lectures in Mathematics, Am. Math. Soc. (1991).
111. L. C. Evans, H. M. Soner and P. E. Souganidis, *Communs pure appl. Math.*, to be published.
112. R. Kokayashi, in *Computing Optimal Geometries* (edited by Jean E. Taylor) Selected Lectures in Mathematics, Am. Math. Soc. (1991).
113. E. A. Holm, J. A. Glazier, D. J. Srolovitz and G. S. Grest, *Phys. Rev. A* **43**, 2662 (1991).
114. Henk Van Beijeren, K. W. Kehr and R. Kutner, *Phys. Rev. B* **28**, 5711 (1983).
115. M. Kotrla and A. C. Levi, *J. Stat. Mech.* **64**, 579 (1991).
116. B. Derrida, J. L. Lebowitz, E. R. Speer and H. Spohn, *J. Phys. A* **24**, 4805 (1991).
117. J. D. Gunton, in *Phase Transitions and Critical Phenomena* (edited by C. Domb and J. L. Lebowitz), 8B, pp. 335–339. Academic Press, New York (1983).

118. M. K. Phani, J. L., Lebowitz, M. H. Kalos and O. Penrose, *Phys. Rev. Lett.* **45**, 366 (1980).
119. P. S. Sahni, G. Dee, J. D., Gunton, M. Phani, J. L. Lebowitz and M. Kalos, *Phys. Rev. B* **24**, 410 (1981).
120. J. E. Taylor and J. W. Cahn, *Acta metall.* **34**, 1 (1986).
121. J. E. Taylor, *Proc. Symp. Math.* **44**, 379 (1986).
122. W. C. Carter and C. A. Handwerker, submitted to *Acta metall. mater.*
123. D. Hoffman, in *Computing Optimal Geometries* (edited by Jean E. Taylor) Selected Lectures in Mathematics, Am. Math. Soc. (1991).
124. F. Almgren, in *Computing Optimal Geometries* (edited by Jean E. Taylor) Selected Lectures in Mathematics, Am. Math. Soc. (1991).
125. E. Yokoyama and R. F. Sekerka, submitted to *J. Cryst. Growth*.
126. J. S. Langer, *Science* **243**, 1150 (1989).
127. D. Kessler, J. Koplik and H. Levine, *Adv. Phys.* **37**, 255 (1988).
128. S. R. Coriell, G. B. McFadden and R. F. Sekerka, *A. Rev. Mater. Sci.* **15**, 119 (1985).
129. G. B. McFadden, R. F. Boisvert and S. R. Coriell, *J. Cryst. Growth* **84**, 371 (1987).
130. R. Almgren, in *Computing Optimal Geometries* (edited by Jean E. Taylor) Selected Lectures in Mathematics, Am. Math. Soc. (1991).
131. K. Tsiveriotis and R. A. Brown, *Int. J. numer. meth. Fluids*, in press.
132. A. Wheeler, W. J. Boettinger and G. B. McFadden, *Phys. Rev. A*, to be published.
133. J. Strain, *J. Comput. Phys.* **85**, 342 (1989).
134. J. Sethian and J. Strain, *J. Comput. Phys.*, to be published.
135. J. Strain, Free-Space Crystal Growth, in preparation.
136. A. Roosen and J. E. Taylor, Simulation of Crystal Growth with Faceted Interfaces, *Interface Dynamics and Growth MRS Symp. Proc. Ser.* Vol. 237 (edited by K. S. Liang *et al.*), in press.

APPENDIX

Glossary

A function is C^2 if it is continuous and all its first and second partial derivatives are continuous functions. It is C^n if its derivatives up to n th order are continuous. A surface is C^2 if it is locally the graph of a C^2 function.

A real-valued function f which satisfies $f(r\mathbf{x}) = rf(\mathbf{x})$ for all $r \geq 0$ is called *positively homogeneous of degree 1*.

A real-valued function f is called *convex* if $f(a\mathbf{x} + b\mathbf{y}) \leq af(\mathbf{x}) + bf(\mathbf{y})$ for all \mathbf{x}, \mathbf{y} and all positive a, b . It is *strictly convex* if $f(a\mathbf{x} + b\mathbf{y}) < af(\mathbf{x}) + bf(\mathbf{y})$ for all non co-linear \mathbf{x}, \mathbf{y} and for all positive a, b with $a + b = 1$ (the latter condition is unnecessary if f is also positively homogeneous of degree 1).

A function f is called *Lipschitz* if there is a constant L such that $|f(\mathbf{x}) - f(\mathbf{y})| \leq L|\mathbf{x} - \mathbf{y}|$. A Lipschitz function is differentiable almost everywhere, but it can have infinitely many points where it does not have a derivative. In particular, its graph can have "angles" in it. It must, however, be continuous and have slopes bounded by L .

Almost everywhere means except on a set of measure zero. It is thus a term which depends on the measure one is using; if this is not specified, then the measure is usually assumed to be the usual n -dimensional Lebesgue measure (length, area or volume, when n is 1, 2, or 3).

A *rectifiable path* or *curve* is an image of a Lipschitz function defined on the unit interval, i.e. a *path* is the set of points \mathbf{x} such that for some function f , $f(s) = \mathbf{x}$ for some $0 \leq s \leq 1$, and it is rectifiable if that function f is Lipschitz. The function f gives a parametrization of the path. Rectifiable paths have tangent directions almost

everywhere and hence are suitable for path integration of functions that depend on tangent direction.

Isotropic means a function does not depend on normal direction. *Anisotropic* means the function is different in different directions.

A specific surface free energy function γ is called *crystalline* if its Wulff shape W_γ is a polyhedron (i.e. its surface is composed entirely of a finite number of flat plane segments).

The *Wulff shape* $W = W_\gamma$ for a surface free energy function γ is defined by

$$W = \{\mathbf{x} : \mathbf{x} \cdot \mathbf{n} \leq \gamma(\mathbf{n}) \text{ for every unit vector } \mathbf{n}\}.$$

The limiting outward growth shape W_x is

$$W_\infty = \{\mathbf{x} : \mathbf{x} \cdot \mathbf{n} \leq M(\mathbf{n}) \text{ for every unit vector } \mathbf{n}\}.$$

A *support plane* for a convex body B is a plane $\{\mathbf{x} : \mathbf{x} \cdot \mathbf{n} = s\}$ such that $\mathbf{y} \cdot \mathbf{n} \leq s$ for every \mathbf{y} in B and $\mathbf{y} \cdot \mathbf{n} = s$ for some \mathbf{y} in B . It touches B but only on its boundary; if B has a tangent plane at \mathbf{y} , then the only support plane for B through \mathbf{y} is that tangent plane.

Smooth in this paper is usually taken to mean C^2 . It is used mathematically to mean more or less "a sufficient number of derivatives for the problem at hand." (Sometimes in other papers it means having a Taylor series expansion at each point which converges to the function in a neighborhood of that point, which is called being *analytic*).

A *piecewise C^2 curve* is a continuous curve composed of a finite union of curves, each of which is C^2 . It can have discontinuities in slope and curvature, but it must be continuous. A *piecewise C^2 surface* is a continuous surface that is composed of a finite number of pieces of surface, each of which is C^2 and each of which has a piecewise C^2 boundary. A *piecewise C^2 function* is one which is continuous, has a piecewise C^2 domain, and the function is C^2 on each piece.

A *geometric growth problem* is defined in Section 1. A function $F(\mathbf{x}, t, \mathbf{p}, X)$ is *geometric* if and only if

$$F(\mathbf{x}, t, \lambda \mathbf{p}, \lambda X + \sigma \mathbf{p} \otimes \mathbf{p}) = \lambda F(\mathbf{x}, t, \mathbf{p}, X), \quad \lambda > 0, \sigma \in \mathbf{R};$$

here $\mathbf{p} \otimes \mathbf{p}$ means the matrix whose ij th entry is $p_i p_j$. The lack of dependence on $\mathbf{p} \otimes \mathbf{p}$ means that the velocity doesn't depend on the second derivative of u in the normal direction, which is reasonable since that second partial has no influence on curvatures.

The function $F = F(\mathbf{x}, t, Du, D^2u)$ is *degenerate elliptic* if

$$F(\mathbf{x}, t, \mathbf{p}, X + Y) \leq F(\mathbf{x}, t, \mathbf{p}, X)$$

for any Y which is a real symmetric matrix with non-negative eigenvalues.

wmc is used to stand for "weighted mean curvature." It is defined for smooth γ and smooth surfaces in Section 2 under the mapping method, and for crystalline γ under the description of the crystalline method. It is discussed extensively in the companion paper to this overview [34].

A 2-dimensional *manifold* is locally an ordinary smooth piece of surface everywhere, with no triple junctions or self-crossings.

The concept of a *varifold* plays two roles. First, it is a mathematical idealization of a surface with fine-scale faceting. Secondly and quite independently, the definition of the first variation of a varifold, and thereby its mean curvature, can handle triple junctions and point junctions without them being part of the mathematical boundary of the surface [34]; this is an essential feature of Brakke's definition of motion of a varifold by mean curvature. Mathematically, a varifold is a "Radon measure on $\mathbf{R}^n \times G(n, m)$." See Taylor [34] and Allard [98] for more details. It can make mathematically precise the notion of "infinitesimal corrugations" because it separately measures where the surface is (the \mathbf{R}^n part) and where the "tangent planes" are [the $G(n, m)$ part], and one can think of it as a

probability distribution of tangent planes at each point on a surface.

A *level set* of a function f is a set of all the points \mathbf{x} such that f takes a certain value on each \mathbf{x} . For example, the 0-level set is $\{\mathbf{x}: f(\mathbf{x}) = 0\}$.

A *shock* must occur whenever characteristics cross. See Section 3.1. Shocks give rise to edges and corners in the evolving surface. A *shock surface* is the locus of points where the resulting edges and/or corners have been (or will be).

A *fan* (or *rarefaction wave*) of characteristics must be introduced whenever the mobility function M is not differentiable, or when the surface is not differentiable (i.e. at corners and edges). See Section 3.1.

A curve or a surface is *embedded* if it has no self-intersections but rather is topologically an ordinary curve or surface everywhere.

A function N on R^3 is a *norm* if and only if it satisfied the two properties of positive homogeneity of degree 1 and convexity. (Strictly speaking, it is often further required that $N(-\mathbf{p}) = N(\mathbf{p})$, but this property of the norm

is not used in this paper.) The *unit ball* of a norm N is $\{\mathbf{p}: N(\mathbf{p}) \leq 1\}$. The *dual norm* N^* to a norm N is defined by $N^*(\mathbf{x}) = \sup_{\mathbf{p}} \mathbf{x} \cdot \mathbf{p} / N(\mathbf{p})$.

The *tangent cone* to a surface C at a point \mathbf{x}_0 is the set of all the rays from \mathbf{x}_0 tangent to C_0 , translated to the origin. That is, it is

$$\{\mathbf{y}: \text{there exist } s_k \downarrow 0 \text{ and } \mathbf{y}_k \rightarrow \mathbf{y} \text{ with } \mathbf{x}_0 + s_k \mathbf{y}_k \text{ in } C_0\}.$$

The *subgradient* of $\gamma(\mathbf{n})$ is defined [78] as the set of all convex combinations of limits of gradients as \mathbf{n}_i approaches \mathbf{n} .

The *crystalline method* is the naturally polyhedral way to treat various equilibrium and growth problems which applies when the Wulff shape is completely faceted. See Section 3.3 and the following paper [34].

A level set to a solution u for a PDE is said to *have an interior* at time t if the set on which $u(t, \cdot) = 0$ is not the lower dimensional object (e.g. curve in the plane, surface in 3-space) that one would expect, but rather is of the same dimension as the ambient space. See Section 2(8).